Chapter 8
Signals in the Soil: Subsurface Sensing

8.1 Introduction

Soil is a primary resource in agriculture. Soil fertility is ability of a soil to sustain the plant growth. Several physical (particle size, structure, water, etc.), chemical (mineralogy, organic matter, and acidity, etc.), and biological properties (beneficial organism) are used by the scientist to describe soil fertility (see Table 8.1). It is important to know these properties of soil fertility in order to optimize the plant production. However, complex nature of the soil makes it difficult to assess the soil fertility. Soil properties may vary on micro or macro level. Micro-variability is due to granularity of the soil. Macro-variability is due to the climate, parent material, time, and how human treats the soil [93]. Soil properties show various spatial and temporal variations. Observing soil in different areas within the field or between multiple fields to study its spatial variations is known as soil survey. Studying the temporal variations refers to the soil monitoring [41, 166].

Traditional approach to investigate soil fertility involves manual collection of soil samples from the field and analyzing them in laboratories. This method specially applies to study the chemical properties and soil texture. However, manual sampling of soil is time intensive, requires a lot of labor work, and highly expensive. Due to these drawbacks, studying spatial and temporal properties of soil, using traditional approach, does not make digital agriculture a viable farming method. The implementation and widespread of digital agriculture rely on use of fast and cost-effective methods [169, 190].

Another approach to study soil properties is to use sensor-based technologies. Soil sensors collect the data for sensing chemical, biological, and physical properties directly from the field. However, due to the complex nature of the soil, only few sensor systems have been successful for use in agriculture. Complex nature of soil makes it difficult to separate the sensor stimuli. The minerals components in the soil cause the mechanical stress and wear in the sensor. Soil absorbs or attenuates most of the EM spectrum due to which remote sensors receive signal from the surface

A. Salam, U. Raza, *Signals in the Soil*,
https://doi.org/10.1007/978-3-030-50861-6_8

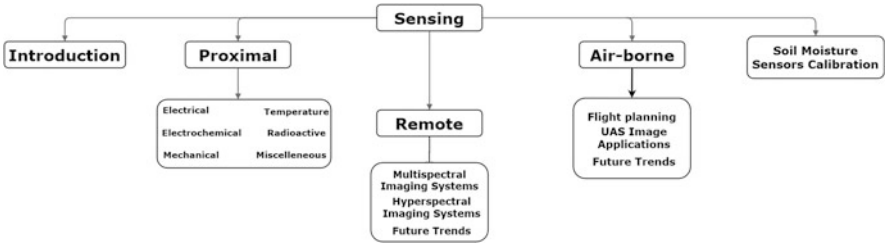

Fig. 8.1 Organization of the chapter

of the soil only. Hence, the success of mapping soil through remote sensing is very limited. Sensing has always been a key technology in the farming industry. In earlier days, farmers used to evaluate the crop properties manually by assessing each plant individually. They used to estimate yield potential, identify stresses from specific symptoms, differentiate water deficiency from nutrient deficiency, and identify diseases from insect infestation. Modern farmers are no different than their ancestors, however, scale of the crops is a major concern nowadays. Farmers, in old days, used to manage small portion of the land, e.g., some fraction of the hectare, however, modern farmers may have to manage hundreds even thousands of hectares of fields. Large field size makes it impossible to manually analyze and manage them. Hence, farmers are becoming increasingly reliant on sensors in their day-to-day farming operations [164, 210] (Fig. 8.1).

In this section we are going to discuss different types of sensor technologies that can be used in monitoring of soil and crop conditions.

8.2 Current Challenges in Sensor Development

EM-based crop canopy sensors have high potential to improve N-fertilizer management, however, some factors may influence its accuracy. These factors may include sensors' operating characteristics (wavelengths and VIs), seasonal variations, genotype effects, and stresses [167, 173]. N-fertilizer management, using proximal crop canopy sensors, assumes that the effect of other stresses, e.g., water, insects, and nutrient, is either absent or equally present in reference and target area, thus, canceling the effect of each other. Even in the irrigated environments, water stress can confound N management during the critical times of the growing season. Some VIs are found to be successful differentiating between N stress and water stress [26]. These indices include three wavebands in the equation (eq. 1) namely the canopy chlorophyll content index [57], the DATT index [39, 141], and the MERIS terrestrial chlorophyll index [38, 157]. However, these three indices are currently not available in any of the commercially available crop canopy sensor system.

Most of the research with proximal crop sensors is being done in N-fertilizer management. However, there is a huge potential of application of proximal crop

sensor in identifying other stresses. Few commercial systems are available which identify plant stresses other than the N stress. WeedSeeker spray system [87] uses the same sensors as GreenSeeker system. It successfully finds the weed in the crop and applies herbicides on the go. WeedSeeker system successfully solves the weed infestation problem in cotton [170, 195]. Salam [151] and Slaughter et al. [187] studies machine vision-based weed detection and control systems using reflectance with the crop sensor for real-time weed control. Crop canopy sensor can also be used in disease and insect detection. High-resolution and multispectral imagery is used to detect disease onset in wheat. Feng et al. [63] use visible to red-edge bands (580–710 nm) to inspect powdery mildew infestation during growth season. Hyperspectral imaging is used to detect damages in sugar beet due to nematodes and fungal pathogens [79]. In Bravo et al. [24], authors used multispectral fluorescence images for the detection of foliar diseases in winter wheat. Huanglongbing disease in citrus canopy is detected by using the ratio of yellow fluorescence to simple fluorescence.

Another trending current of area of research is the concept of sensor fusion. Sensor fusion refers to using multiple proximal crop sensors over single sensor. Combining various sensing techniques can give more accurate measurements promoting the widespread adoption of sensor-based technologies from crop management [5, 150]. Veris Technologies combines multiple sensors for soil electrical conductivity (EC), pH level of the soil, and soil organic matter to a single platform [209]. Salam and Vuran [164] and Shiratsuchi et al. [186] use three different types of sensors: optical for canopy reflectance, thermal for temperature, and ultrasonic distance sensor for height, to assess the N status in the crop. The authors in [213] combine four different sensors to study the herbicide dosage control. Sensor fusion in [108, 197] documents the information about crop and straw yield and grain protein content for stress evaluation in harvesting wheat. Salam [142] and Lamb et al. [103] use the combination of active and passive sensors to map a cotton field. Sensor fusion is also used to study high throughput phenotyping. A sensor fusion system for field phenotyping in [28, 148] integrates a color camera, Light Detection and Ranging (LIDAR), time-of-flight cameras, light curtain imaging systems, and a hyperspectral imaging sensors. The system could measure plant moisture, lodging biomass yield and tiller density. High throughput phenotyping platforms [10, 154, 210] use multispectral active crop canopy sensors, LIDAR or ultrasonic sensors, and thermal sensors. Crop Circle Phenom [85, 210] incorporates sensors for canopy temperature, humidity atmospheric pressure, air temperature, and canopy reflectance wavelengths of 670, 730, and 780 nm.

8.2.1 Proximal Sensing

The term proximal indicates the close proximity of the sensors to the crops. They are deployed close to the crops; thus, different from remote sensors. Due to advancement in unmanned aerial systems (UASs), which used to be a remote

sensing technique, is now considered as a proximal sensing technique. We consider the proximal sensors as the sensors which determine and evaluate the crops' properties ranging from physical contact with canopy to a few meters above the canopy [165, 172].

Crop producers are interested in the properties which may influence yield and quality, and issues which can be detected and managed during crop producing seasons. Some of the properties that may interest a farmer include biomass accumulation, water status, nutrient deficiency (particularly nitrogen), disease onset, and insect infestation. Monitoring these properties is crucial during some specific periods of growing seasons. Remote sensing, e.g., aerial platforms, is easily affected by weather and clouds condition limiting their use. However, proximal sensing is not affected by these making it an appropriate choice during growing season [165, 172].

- **Contact or in-situ sensors:** Some sensors are either directly attached or placed among the plants. Sap flow sensors, attached to the stem of the plant, are used to estimate transpiration [149, 171, 191]. Ground-based sensors are used to measure leaf area index (LAI) [25, 144]. However, measuring sap flow and LAI with static instrument is a time-consuming process. Crop-meter [56, 170] is a simple biomass sensor for the cereals which works on the pendulum principle. Crop-meter is mounted on vehicle driven through the crops. If crops' biomass is higher, crop-meter is highly deflected.
- **Ranging Sensors**: Range-finding or distance measurement is another approach to find biomass and height of the crop. Salam [148] and Dworak et al. [55] measure the biomass, characteristics of the canopy, and crop stand using acoustic and electromagnetic (EM) wave ranging. Geometric characteristics of the citrus trees can be quantified by laser scanner. It is used for yield prediction, measurement of water consumption, health, and long-term productivity monitoring of the crop [104]. Water stress in maize can be detected by integrating acoustic ranging sensors with multispectral and thermal sensors [162, 186].
- **Electromagnetic (EM) Sensors:** Most of the crop canopy sensors use EM spectrum. EM sensors can be classified as active-with internal energy source, or passive-using external emitted energy source. The four regions of interest in EM spectrum include visible, near-infrared, mid-infrared, and thermal infrared ranging from 400 nm (visible) to 14,000 nm (thermal infrared) [100, 143]. The properties of the plants, e.g., plant pigment concentrations, cell structure, water content in canopy and leaves, are determined by reflection or transmission in these spectrum ranges. Reflectance does not give much information about plant stress. Vegetation index (VI) allows to infer the plant stress and specific properties of plants by using the relationship between or reflectance in multiple spectral regions. Among 150+ VIs, the most famous VI is normalized difference VI (NDVI) [138, 197]. NDVI is calculated using following equation:

$$\text{NDVI} = \frac{(\text{NIR} - \text{RED})}{(\text{NIR} + \text{RED})} \tag{8.1}$$

Chlorophyll meter, frequently used instrument in the plant research, is used to measure the chlorophyll content in a plant. It is based on the reflectance meter presented by Wallihan [212]. Konica Minolta SPAD 502 Plus [118] is a commonly used and mostly available chlorophyll meter today. The meter is used in determining chlorophyll concentration [113] at 650 and 940 nm of wavelengths. The performance of this meter has been studied [113] for determining the chlorophyll content and ability to detect N stress and, assuming the high correlation between chlorophyll and nitrogen content in a plant, consequently predict the demand for N fertilization [22, 27, 152, 179].

The Dualex Scientific [51, 154] is another handheld senor which measures the chlorophyll and polyphenol contents in ultraviolet, visible, and NIR wavelengths. Polyphenols can be used to determine plant stress factors such as N availability [157, 173]. When used together, Dualex and SPAD meter are more sensitive in calculating the corn N status rather than being used alone. Force-A also manufactures the handheld sensors used to determining abiotic stresses in the plant especially in detecting disease [145, 151, 161, 175].

Chlorophyll meters are useful in estimating the properties of a given plant, however, it becomes laborious to measure the properties of a group of a plants or fields. It is a useful proximal sensing tool for a plot of small size. However, the labor challenges associated with the chlorophyll meter prevent it to be used by the farmers for N-fertilizer management.

- **Mobile EM Sensors:** Yara N-Sensor [150, 223] is a passive spectrometer system that can be mounted on a tractor. It consists of two spectrometers which are used to scan crop canopy and real-time correction of the reflected signal in a wavelength selected between 450 and 900 nm [159, 173, 226]. NDVI and various other VIs are calculated through reflectance. The system then adjusts the application rate of N fertilizers for scanned region in real-time. N-Sensor is majorly used for spatial N management of wheat [21], however, its applications are also found in corn [156, 202] and potato [155, 226].

  Passive sensors face the challenges of clouds, angle of the sun, and time of the day. Active sensors have been developed to address the challenges of passive sensors. Active sensors, as discussed earlier, use internal light source [42, 160]. Optical sensors, a type of proximal active sensors, use radiometric principle. Holland et al. [84] discuss how this principle, especially inverse square law of optics, affects the functionality and use of the sensor. Salam [153] and Raun et al. [132] showed that, as compared to the traditional methods, sensor-based N application methods can increase the nitrogen use efficiency (NUE) by 15%. This system was developed by Oklahoma State University and was named GreenSeeker. GreenSeeker system [87, 168] is an active crop canopy sensor system commercially available for the N-fertilizer management. It uses an in-field reference for the calibration of the sensor for specific field conditions. It measures reflectance at the wavebands of 671 ± 6 and 780 ± 6 nm. The system generates the response index (RI) by dividing the in-field reference NDVI by targets' NDVI. RI and in-season estimate of yield (INSEY) are used in various crop and locale specific algorithms to generate the real-time fertilizer N rate.

This system can be used for many crops, however, majorly used for corn [2, 169] and winter wheat [147, 196]. Handheld version of this sensor has also been developed by Trimble for the exploration purposes. It comes with an integrated power supply datalogger and GPS.

Crop circle suite of sensors, initially developed by Holland Scientific as ACS-210, is set of active crop canopy sensor. ACS-210 is two-band active sensor which measures reflectance at 590 ± 5.5 and 880 ± 10 nm. It is not used commercially anymore and is replaced by various other three-band sensors such as ACS-430 and ACS-470. They also have handheld sensor, RapidScan CS-45, equipped with a datalogger, power supply, and a GPS. It has the optics similar to ACS-430.

The set of sensors described above are primarily used for the research purposes. Holland Scientific has integrated the technology into OptRx®crop sensor system [152, 192] for the commercial use. OptRX uses the ACS-430 and measures the reflectance at wavebands of 670, 730, and 780 nm. OptRX, like GreenSeeker system, uses in-field calibration. OptRX is designed to be used with a universal N recommendation algorithm which can either be adjusted by the user [82, 162] or virtual reference approach [83, 144]. In virtual reference approach, healthiest area of the field is selected as a reference N status of the crop and the area is scanned in real-time. This prevents the grower to establish a nitrogen rich area as a reference strip in the field. Yara N-Sensor ALS (active light system) uses xenon flash lamp as a light source. CropSpec system uses laser as a light source and measures reflectance at 730–740 nm and 800–810 nm bands. The operating characteristics of both, CropSpec and N-Sensor ALS, are similar to those of passive N-Sensor.

Sensors sense analog physical or chemical stimuli, e.g., temperature, heat, etc., and convert them to a digital signal for further analyses. Data analysis methods are used to get information from this data and finally incorporated in decision making to take appropriate agricultural decisions. As discussed in previous section, complex nature of soil requires sensors to be placed in the soil at very short distance from the soil. Proximal sensing is highly effective in creating high-resolution soil maps. Salam and Shah [163], Salam et al. [172], and Rossel et al. [137] define proximal sensing as the application and development of sensor that operates close by or inside the soil. A proximal soil sensor system ranges from simple stationary systems with one or more sensors and data recording and transmission unit to complex automated and mobile systems. Complex proximal system may be equipped with a platform to carry sensors, sampling unit, sample heads, sample preparation equipment, and GNSS.

8.2.1.1 Future Research Directions

Proximal sensing is used to achieve sustainability and reducing the environmental impact that may occur due to crops. Proximal sensing enables spatial management and manages temporal variations for the site-specific management in precision

Table 8.1 Soil properties relevant for plant production as indicated by the notion of soil fertility [69]

Physical	Chemical	Biological
Particle size: gravel, sand, loam, clay	Mineralogy: quartz, clay type	Mineralization fixation
Water: water content, water potential	Organic matter: total content, fractions (labile, stable)	Beneficial organisms
Structure: bulk density, porosity	Nutrients: total content, plant available (e.g., N, P, K)	Bioturbation by animals and plants
Thermal properties: thermal diffusivity, heat capacity, heat conductivity, specific heat	Acidity pH	
Relief: slope, exposure	Redox potential: O_2	
	Toxic substances	

agriculture. Proximal sensors allow an efficient use of resources by detecting and taking preemptive measures in a timely manner.

There is a huge research potential in developing active proximal sensors for use with UAV. Apart from N stress, it can be used to explore water and nutrient stress and many other diseases. There is potential to study different stresses using multispectral fluorescence, mid-infrared, and thermal region of EM spectrum. Non-EM sensors, e.g., pheromone and spore detectors can be investigated for disease or insects.

8.2.2 Electrical Soil Sensing

Some sensors use electric circuits to measure the electrical conductivity (EC) of a soil, capacity of the soil to become polarized, or form magnetic fields. Such sensors are known as electrical sensors [105, 143]. Electrical sensors are assessed in the frequency range of 0 (direct current) to 300 (radar) GHz. Electrical sensors are the most common proximal soil sensors. In the next section, we discuss relevant electrical properties of soil [99, 178].

8.2.2.1 Electrical Soil Properties

Electrical conductivity (EC) of a soil refers to the amount of salt in the soil (salinity). It indicates the health of the soil. EC affects the crop growth, crop suitability, and plant nutrient availability (RSEC). EC in soil can be due to movement of free electrons, movement of ions in dissolved water, and surface conductivity [99]. EC due to all three mechanisms is known as bulk electrical conductivity (ECa). The ECa is mainly associated with the properties of soil such as: water content, hydraulic permeability, temperature, bulk density, and surface changes. In non-saline soils,

spatial variations of soil ECs within the field are due to the soil texture. Coarse sands have limited contact and low capacity of holding moisture, hence are poor conductors. Heavy clays have high capacity of holding moisture and high particle contact, hence are good conductors.

Tendency of a medium to become polarized upon passing electricity is its dielectric permittivity [159, 178]. Dielectric permittivity increases with the decrease in frequency. Soil sensors measure the permittivity at frequencies between 1 MHz and 1 GHz. It is used to measure the soil–water content. Dielectric permittivity of free water is 80 [155, 178]. The electromagnetic sensors cannot measure the dielectric permittivity of the soil directly. They use the travel time or frequencies to derive the values. As a result, other interfering soil properties (ECs, temperature, magnetic permeability, and signal frequency) are also taken into account while measuring these properties [61, 119, 158].

The ability of the soil to form a magnetic field is known as magnetic permeability. Ferromagnetic compounds such as iron oxide and super paramagnetic minerals can be found in the soil due to atmospheric deposition and human activities [75, 100, 119]. If present, the magnetic permeability is proportional to the volume of these compounds. Many proximal sensors measure soil susceptibility which is the ratio of mediums' permeability to permeability of free space minus one. Magnetometers or EM sensors are used to measure the magnetic properties of the soil. Magnetic properties of soil, both susceptibility and permeability, are mainly used in the field of environmental pollution and archeology [75, 165]. Very limited work has been published on the use of magnetic properties in soil mapping from agricultural context [15, 171]. All of the above three properties are highly dependent upon the frequency of applied EM field. Lower frequency methods are more related to EC and high frequency methods, e.g., TDR and radar, are more associated with dielectric and magnetic permeability.

8.2.2.2 Electrical Soil Sensors

Galvanic coupled resistivity (GCR) measures the bulk electrical resistivity (ERa) in Ω-m under the low frequencies of less than 50 Hz. High frequencies can be used to analyze polarization effect. It uses two electrodes, in direct contact with the soil, and an ohmmeter to measure the electricity resistance by the soil. Wheatstone bridge uses four electrodes, in pair of two, to measure more accurate readings. One pair is used to inject electric current into the soil and the other is used to measure the potential difference. GCR is a relatively cheap, robust, and low power method of measuring electrical resistivity. Contrary to other electrical methods, GCR is less sensitive to electromagnetic sources. Main disadvantages of GCR are that it requires good contact with the soil and the invasive nature of galvanic coupling. The performance of electromagnetic induction (EMI) methods is much better in frozen, stony, or dry soils as compared to GCR methods [149, 211].

Electromagnetic induction (EMI) sensors are greatly impacting the digital agriculture [37, 77]. It uses two electrical coils (solenoids) and operates at the

frequencies of 100–60 kHz (0.4–40 kHz, [37, 146]). On applying alternating current (AC) to the transmitter coil, an EM field termed as primary field is generated. This primary field induces an eddy current through the soil, which results in a secondary field. The secondary field differs from primary field in terms of amplitude and phase [116, 153]. The phase and amplitude difference between primary and secondary field depends upon various soil properties [12, 145], spacing between the transmitting and receiving coil, distance between and coil and soil surface, and orientation of the coils. ECa is calculated by using amplitude and phase differences between primary and secondary fields, and inter-coil spacing. Tuller and Islam [203] study the magnetic susceptibility of the soil. However, few studies in agriculture use it.

Capacitive methods use the capacitor principle to analyze the soil properties. Electrical oscillator is connected to electrode at the frequency of 0.1–0.25 GHz (38–150 MHz) to create an electric field penetrating the dielectric medium (soil). The dielectric permittivity of the soil can be determined by estimating the charging time of the capacitor with that medium [121, 156]. FDR and capacitance probes are mostly used for measuring the water content in the soil. Both are sensitive to clay and temperature variation of the soil. However, they are cheaper with a flexible electrode geometry. Mobile mapping of ERa is also one of the applications of capacitance principle. Capacitive coupled resistivity (CCR) is based upon classical GCR method with only difference of using capacitive plates/antennae instead of galvanic electrode [102, 160].

Time-domain reflectometry (TDR) is used to determine the water content of the soil by measuring the travel time of electromagnetic waves through the soil under high frequencies. The travel time is used to measure the dielectric permittivity of the soil which in turn is used to measure the soil–water content. TDR sends the electromagnetic signals via two electrodes buried in the soil. It measures the propagation velocity of a step voltage with a bandwidth around 20 kHz to 1.5 GHz [135, 161]. TDR is less affected by the interference due to EC because they operate at frequency >0.5 Hz.

Other variants of TDR and FDR are also used as electrical measurement methods. Some of them discussed briefly in [121] includes amplitude domain reflectometry (ADR), phase transition, and time-domain transition (TDT).

8.2.2.3 Stationary Electrical Sensors

Stationary soil sensors are very useful in monitoring soil–water properties. It has advantage over traditional methods, e.g., tensiometers, in having high range of tension (up to 1500 Pa), ability to be placed for long time, and low cost. However, slow reaction and intervention of soil salinity are some of the disadvantages [54, 168].

Stationary soil sensors must be carefully calibrated to get the correct measures [61]. Even a small scale variation can cause several problems. Durner et al. [54], for example, perform an experiment with 107 sensors on 60 m^2 test site. Sensors

readings were varied significantly over the two months due to small scale variation (growth of algae) in the soil surface. It is difficult to distinguish the effect of water on electromagnetic properties from other factors such as salinity, bulk density, etc. [90]. It is recommended to use standard procedure, multiple sensors, and rain gauge records for detection of error and troubleshooting [54, 146, 197]. Salam et al. [172] and Muñoz-Carpena et al. [121] present a detailed survey of various commercially available soil sensors. Some sensors are briefly described in coming section.

- **Stationary TDR and capacitance sensors** can be used for stationary measurements. TDR uses metal rods and capacitance sensors are flexible and cheap. TDR gives more accurate reading under high frequencies, however, comparative studies suggest mixed results [61, 148, 162]. Durner et al. [54] studied 15 different types of sensors (FDR, TDR, capacitance) and posited that most sensors respond to temporal changes reasonably well, however, with a considerable difference in absolute values.
- **Gypsum Block method** is another method to assess the soil–water content. Apparatus contains a porous block with embedded electrodes. In an ideal scenario, the soil–water content and the bock water should be uniform. Fiber glass and gypsum can be used as a porous block. Gypsum is a cheaper option but it needs calibration and it decomposes with time. Fiberglass is durable and gives more stable calibrations. The simplest implementation consists of a gypsum block with two wires connecting to resistivity meter.
- **Electrical resistivity tomography** is a method which is used to study the depth profiles and spatio-temporal properties of soil–water content in high resolution. It extends GCR method with array of multiple electrodes (20–100) placed equidistantly in a transect. Four of the electrodes placed at different locations and spacing are switched on to study the depth variations[94, 210, 211].

8.2.2.4 Mobile Electrical Sensors

Mobile electrical sensors were the first sensors used to measure the soil spatial variability in digital agriculture [151, 161, 174]. EMI and GCR based sensor systems are still the most commonly used systems in digital agriculture. Salam [150, 158] and Gebbers et al. [70] did a comparative study on GCR, EMI, and capacitive coupled sensors which is discussed in the coming section.

- **Galvanic coupled resistivity** Mobile GCR sensors, use four-point method, consist of four wheels acting as electrode. Four-point arrangement is extendable by adding more pair of electrodes to get the readings at different depth variations. Depth sensitivity is controlled by the spacing and position of electrodes. The most common arrangement of the electrode is Wenner array equally spaced electrode in a straight line. Veris 3100 uses injected current of 100 mA and frequency of 150 Hz and works with the two depths [193]. Six rolling electrodes are arranged in Wenner array. Spacing between the electrode is 24 cm for the shallow and 72 cm for the deep measurement. Automatic resistivity profiling (ARP) is made

by Geocarta company in France. It operates at frequency of 225 Hz and arranges the rolling electrodes in trapezoid pattern [174]. The spacing between the current electrode is 1 m and that of between voltage electrode is 0.5, 1, and 2 m. GEOPHILLUS is an advance system from Germany operating at the frequency of up to 1 kHz [111, 142]. It uses 6 pairs of galvanic coupled electrodes arranged in an equatorial dipole–dipole array. First pair measures the electric current while other 5 pairs measure the voltage drop simultaneously.

- **Electromagnetic induction (EMI)** EM38 instrument from Geonic Ltd., is one of the most popular mobile electromagnetic instruments in digital agriculture. Salam and Vuran [166] and Heil and Schmidhalter [77] recently gave the review of EM38 applications. Orientation and spacing of the coil, and frequency often affect the DOI characteristics. EM38 uses the inter-coil spacing of 1 m and provides the readings for magnetic susceptibility and electrical conductivity simultaneously. EM38-DD with the same inter-coil spacing uses two EM38. EM38-MK2 operates at frequency of 14.5 kHz and uses three coils with two receiver coils separated by 0.5 and 1 m from transmitter coil. Topsoil Mapper (Geo-prospectors, Traiskirchen, Austria) is the first EMI instrument which provides various interesting features specially for the digital agriculture. It can be mounted to the front of the tractor because of its ability to suppress interference from the metal. It can be used for the estimation of bulk density, water content, texture, real-time tillage control, and seed rate.
- **Capacitance and CCR sensors** [3, 167] reviews the mobile sensors that use capacitive principle and galvanic coupling. Mobile capacitive coupled sensors (CCR) have been in the market for 10 years, however, their use in agriculture has been very limited. They work better than the galvanic coupled sensors in places where EC is very low and a mechanical contact is difficult. However, places where EC is high, receiver dipoles' voltage becomes too small and its measurements are unreliable [7, 147]. Coaxial cable or metallic conductors are used as a capacitor plates. One pair is used to generate current in the ground and other is used to measure the potential distribution at the surface of ground [102, 165].

  OhmMapper (Geometrics Inc., San Jose, USA (http://www.geometrics.com/)) is a CCR system with capacitive coupling. It can continuously collect the data even at the short time interval of 0.5 s. A coaxial cable is divided into transmitter and receiver sections and both are of 5 m in length. An alternating current is generated by the transmitter at 16 kHz. It consists of a power supply, a datalogger, and rope separating two dipoles from each other. Distance and length of dipoles are used to measure the DOI. Distances can also be set arbitrarily.
- **Mobile TDR and GPR sensors** GPR systems are available commercially in the market, however, only prototype of TDR systems can be found in the literature. Salam [141] and Thomsen et al. [198] study the modified version of stationary TDR with longer probes designed for stop-and-go measurements. For continuous mobile measurement, geometry of the traditional TDR probes needs to be modified along with the consideration of other aspects such as contact and

heating. Due to time taking data analysis, use of GPR in agriculture is for research purpose only. However, it is commonly used in geophysical and archeology.

8.2.3 Soil Temperature Sensors

- **Thermal sensors** One of the oldest sensor systems in agriculture are thermal sensor systems. Electrical and infrared (IR) thermometers are used to measure the temperature. Electrical thermometers need to be in physically contact with soil, whereas IR ones can be used for stand-off readings. Thermistor and thermocouple are the examples of electrical thermometers. Thermistor relies on change in resistance and thermocouple uses the thermoelectric effect. Electrical thermometers are cheaper and are integrated with various sensors systems such as TDR and FDR. An IR thermometer uses a lens to focus on thermal radiations emitted from an object onto a detector. The lens is sensitive in the range of 0.7–1.4 μm. Thermal properties such as volumetric heat capacity, thermal conductivity, and thermal diffusivity can be utilized for the mineralization, germination, and other growth related processes.
- **Heat-pulse sensors** Heat-pulse sensors [29, 163] are primarily used for measuring the volumetric water content. Sensor consists of at least two probes: heater probe and a temperature probe (thermocouple). A heat pulse is applied at the heater probe and the temperature of the soil is measured at the temperature probe. This approach is dependent on the fact that specific heat of the water is higher than the other constituents of the soil. After applying the heat impulse, temperature depends upon the volumetric heat of the soil medium. More water content results in low temperature rise and vice versa. In commercial systems, heater probe and thermocouple are insulated in a porous matrix. Water potential of the soil should be same as of the matrix. By this assumption, the water content of the matrix becomes the indirect measure of the water content of the soil [133, 152]. Heat-pulse sensors have slow response and are sensitive to soil contact. Due to these reasons they are mainly used for the stationary measurements. A very less information is available on the continuous heat-pulse mobile sensors in the current literature. Authors in [9, 159] describe an approach of IR thermometer measuring the temperature variations in soil because of warming up by solar irradiation.

8.2.4 Electrochemical Soil Sensors

Electrochemical sensors are used to measure the chemical properties of the soil, e.g., nutrient content and pH level of soil. Electrochemical sensor can be categorized into potentiometric, amperometric, and electromechanical biosensors. The working principle is based on chemical interaction between the sensor and chemical component

of the liquid. The two most popular methods used for electrochemical sensors are ion-selective electrode (ISE) and ion-selective field-effect transistor (ISFET). The electrochemical sensors for pH use the combination of ISE and ISFET and fall into the category of potentiometer sensors. Salam [157] and Kim et al. [97] extensively review the potentiometer sensors. Their main advantage is that they directly measure the liquids' ions concentration.

The ISE system consists of a sensing membrane (glass, polyvinyl chloride, or metal) and a reference electrode both assembled in a single probe. The potential difference between both electrodes is measured and concentration of selective ions is estimated using Nernst equation (reference for Nernst). ISFET uses field-effect transistor technology along with the selectivity of ISE. The ion-selective membrane acts as a gate electrode and controls the current between the two semiconductor electrodes. ISFET differs from ISE in that it does not have internal solution and the ion-selective membrane is firmly attached on the gate. The pH ISE with antimony membrane is being used in on-the-go commercial systems for pH mapping [5, 100].

8.2.5 Soil Radioactive Radiation Sensors

- **Gamma ray sensors** Gamma rays are produced from decayed nuclei of radioactive elements and have highest energy and lowest wavelength within the EM spectrum [59, 170]. There are naturally occurring nuclides in soil which emit gamma rays in the range of 0.4–2.81 MeV. Large amount of gamma rays is harmful that is why active gamma sensors are avoided due to high energy and ability of penetration into the material. Gamma ray detectors convert the incoming radiation into light photons which are further amplified by photomultiplier and detected by photodetector. Passive sensors detect the gamma photons released from radioactive decay present in the soil. Passive gamma sensing is very good for quick soil mapping because of already established technology, strong theoretical background, and robust instrument that can quickly collect data.

  In proximal sensing, gamma sensors are used as ex-situ systems in both continuous and stop-and-go mode with 90% of the radiations coming from upper 0.3 to 0.5 m of the soil. Bulk density of the soil can affect the readings [112]. Many radionuclides occur naturally in the soil, however, only potassium (^{40}K), uranium (^{238}U), and thorium ^{232}Th are the ones producing gamma rays with sufficient energy and intensity. Radiation not coming from the earth are known as background and mainly come from radon (^{222}Rn) [112].

  Clay (soil texture) is usually correlated with the gamma count because K, U, and Th are incorporated by the major fraction of the clay, i.e., clay minerals [76]. Gamma count has also been formulated through indirect correlation to pH, organic carbon, gravel, and moisture [76, 154]. These indirect relationships are highly dependent upon relation of soil to other properties such as the total K in the soil. These relationships showed high spatial variability which mandated the

separate calibrations for each site. Heggemann et al. [76] proposed a general model for predicting soil texture fractions (clay, sand, silt) from non-linear support vector machine (SVM). Most of the studies counts only three regions (K, Th, Ur) and total gamma counts [137], however, some researchers also recommend to study full spectrum [206]. Though not much performance gains in prediction model are shown when the full spectrum is considered [137, 145].

- **Neutron sensors** Neutron sensors are used to measure the soil moisture. It can be classified as active and passive neutron sensors. Neutron probes (active sensors) use the waters' moderator properties for neutrons. The high-energy neutrons from the sensors collide with the H nuclei of water. The number of neutrons scattered back at the device is directly proportional to the water content in the soil. More water content results in more neutrons scattered at device and vice versa. Neutron probes though accurate, however, are very expensive and their operation is strictly regulated by the law because of radioactive neutron source. Hence, they are rarely in use today.
  Cosmic-ray probes are the passive neutron sensors. They measure the low energy neutron (1 keV) generated within the soil by moderation of cosmic-ray neutrons [32, 171]. This moderation is primarily controlled by the soil–water content. This method provides a continuous and aboveground (without contact) method of monitoring of water content. Cosmic-ray neutron sensor can be used to measure the soil–water content over footprint 600 m and depth varies from 0.76 m (dry soils) to 0.12 m (wet soils). The depth of exploration is highly dependent on soil moisture. Soil moisture is calculated from neutron intensity using a universal function which is indifferent to changes in soil chemistry [32, 155]. Mobile probes, mountable on vehicles, are also designed for in-depth spatial investigation [32].

8.2.6 Mechanical Soil Sensors

- **Cone penetrometers** Vertical cone penetrometer is a device that is used to measure the soil resistance to penetration, i.e., soil strength, as they are inserted to the soil. In agriculture, they have been used for a long time to detect the soil compaction [190]. Some of the soil properties that may affect the index of the cone includes bulk density, soil type, soil moisture, and structure of the soil [48, 164]. In 2000, Veris technologies were the first to design the stop-and-go automated cone penetrometers (Profiler 3000) for soil mapping [50, 144]. However, high variation of penetration resistance makes the soil mapping expensive [48, 149]. Therefore, systems with continuous mapping were more favored.

  There were three main approaches to use: (1) horizontal penetrometers to measure horizontal penetrations [8, 156], (2) use of draft force sensors and

vertical force sensors between tractor and tillage [78], and (3) measuring fuel consumption of tractor during tillage [23]. In a review of penetrometer and draft/vertical force sensors, [78] emphasizes that if soil texture and moisture is known then variation in penetration resistance can be understood in terms of bulk density. Mapping of bulk density has been done using the integrated multi-sensors system in [184].

- **Tensiometers** Tensiometer is the device used to measure the soil matric potential, i.e., soil moisture tension. A matric potential is found in the water when the water in soil is under tension. The name, tensiometer, owes to its ability of measuring tension. It consists of a porous cup connected to manometer through a water-filled tube, vacuum gauge, pressure transducer, or any other pressure measuring device. The plant needs to overcome the tension to pull water from the soil. Tensiometer is advantageous in that they provide direct and easy to interpret measurements. However, its maintenance requirement is high and range of measurement is limited. They need to be protected in frost and embedded properly to establish good contact between porous cup and soil. They are not suitable for operation under -85 kPa and it takes several minutes to establish equilibrium between porous cup and soil matrix. Due to these reason, tensiometer should only be used as stationary sensors [143].

8.2.7 Other Sensors

- **Gas sensors** Gas sensors are becoming popular for detection of acetylene. Plants emit acetylene in unsuitable conditions, e.g., drought or fungal infections. CO_2 emission is analyzed to study the biological activities in plants. Non-dispersive infrared (NDIR) CO_2 sensors are used to detect simpler gaseous molecules such as CO_2, SO_2, and NO_2. NDIR is affected by the cross-sensitivity of these gases in low concentration [95]. Electronic noses are used for assessing the complex molecules [160, 216].
- **Capillary electrophoresis** Capillary electrophoresis (CA) is used to separate solute ions from the liquid soil extract after applying electric field. Soil is put in a capillary tube and ions are identified from their time of travel inside the capillary. The tuning parameter for the setup contains selection of electrolyte solution, capillary's' length, and applied voltage to electrolyte. CA has been a commonly applied method in the labs, however, recent development in making portable systems is also being reported [153, 189]. The iMETOS Mobilab was recently released by Pessl Instruments GmbH. It is based on small and inexpensive microfluidic chip CA and measures to NO_3^-, PO_4^-, and K^+ (Weiz, Austria).

8.2.8 *Integration of Proximal Sensors in Digital Agriculture*

- **Sample preparation for the soil:** Ideally, sampling is not required in proximal sensing. Due to the impact of several properties of soil on sensor, selectivity of a sensor is degraded. Unfavorable soil conditions, e.g., very dry soil, presence of plant residue, are also one of the obstacles in taking measurements. Hence, sample preparation can solve these issues [107, 168]
- **Calibration and measurement errors in soil sensing:** As discussed, sensors are affected by various soil properties. EC of a soil is affected by water, clay content, and salt. In field, measurements can vary beyond control due to soil properties and other environmental factors. Data must be interpreted very carefully. Hence, a traditional lab analysis of the soil is advised for calibration of sensor readings.
- **Sampling design for calibration samples for soil sensing:** Several studies have highly emphasized on the sample calibration for successfully translating the sensor measurement to soil fertility properties. Determining sampling site for the stationary sensors is easy whereas it is difficult for mobile sensors. Adamchuk et al. [4] provide an algorithmic solution and give three criteria for optimal sampling: (1) accounting for spatial separation to avoid readings from auto-correlated samples, (2) increasing spread of value for stability, (3) local spatial homogeneity so that sample fully represents the sampling site instead of being an outlier. Adamchuk et al. [4] and Salam and Vuran [165] also transformed these criteria into mathematical model.
- **Robustness, safety, ease of handling and economic efficiency:** Due to deployment in rough agricultural environment robustness and safety (protected cables and watertight plugs) of proximal sensors is a pre-requisite for daily usage. Some sensors (XRF systems and GCR) can cause serious injuries and operators need to be trained properly as a safety measure. It contributes towards the efficiency and safety of the users.
- **Integrating to decision-making algorithm:** Sensor data alone does not make any sense. It gives information only when integrated into some decision-making algorithm. In digital agriculture, decision support system links the input data (temperature, moisture) to output (crop yield, profitability). These systems can help in decreasing effect of agronomic measures and can be used to do cost-benefit analysis.

Future Trends

Currently, commercially available proximal sensors capture very limited number of soil properties and that too with insufficient accuracy. New proximal sensors systems covering wide range of soil fertility properties and more accuracy are needed. These sensor systems must be affordable and manageable in order for the farmer to be comfortable to use them. Low-cost handheld sensors can be used to introduce farmers to the benefits of using digital agriculture.

A combination of multiple sensors is used to capture different properties of the soil. There is no single platform that combines multiple sensors capabilities. There is a need of establishment of reliable calibration database and protocols for evaluating the sensor data. It also allows to compare the sensors readings. Only few countries offer a scientific sound and robust decision-making algorithms to their farmer for the management purpose. Only ad-hoc approaches are being used in digital agriculture. These approaches have not been validated over a different range of conditions. Authorities have to support and establish guidelines for the promotion of sensor-based farming.

Most of the mobile soil sensor data is evaluated offline. Due to the requirement of quick response in crop management, farmer demands a real-time management. There is a lot of uncertainty about the proper soil sensor usage due to which immediate rate of investment cannot be guaranteed to the farmers. However, digital agriculture must not be evaluated for only its economic potential. A lot of environmental benefits (avoiding pollution and erosion) associated to the adoption of digital agriculture. These benefits must be quantified to support farmers. Farmers and agriculture advisors do not want to waste their time in data calibrating, cleaning, and integration to decision support systems. They need smooth transition of raw data into information for decision making that too with robust and user-friendly systems. These systems must be flexible enough to work with various data formats. Decision support algorithms, e.g., for fertilizer recommendations are based on simple model and require few input parameters. Research in proximal sensing should start out by matching these simple models. However, proximal sensing can provide information which is neglected by the standard algorithms for best management. Advanced soil-crop model can integrate this information for further improvements.

8.3 Remote Sensing

Science of collecting data from the surface of the earth without direct contact is known as remote sensing. Remote sensors are the instruments that collect this information by detecting and measuring the reflected electromagnetic radiations. Platforms used to carry remote sensors include manned aircraft, satellites, and unmanned aircraft systems (UAS). Some sensors can be mounted on ground-based vehicle or may be integrated into handheld systems. Few factors which can be considered for selection of appropriate platform are: size of the area to be imaged, complexity of crop types, time, and cost. Manned aircraft-based sensors are also known as airborne sensors and satellite-based sensors are also known as spaceborne sensors. Different platforms should be evaluated for their suitability of and efficacy for digital agriculture applications [144, 147].

This section provides an overview of airborne imaging system and spaceborne remote sensors being used in digital agriculture. Remote sensors can broadly be categorized into two types: (1) imaging (cameras) and (2) non-imaging (spectroradiometers). Imaging sensors give the vertical (nadir) view of the target area. As with

the proximal sensing, remote sensing is also passive (electro-optical sensors) and active (imaging radar) depending on the source of energy. However, active sensors can take measurement regardless of time of the day and season. Electro-optical sensors are the imaging sensors that detect and convert the reflected radiation to the electrical signals which then can be viewed as images on the computer. Electro-optical can detect the radiations of wavelength ranging from 0.3 to 15 μm. Most of the airborne and satellite remote sensors in digital agriculture are electro-optical sensors. In the coming sections, we discuss the advances in airborne and satellite-based remote sensors along with the examples, advantages, and disadvantages in digital agriculture [145].

8.3.1 Multispectral and Hyperspectral Imaging

8.3.1.1 Multispectral Imaging Systems Using Industrial Cameras

With overall advancement in imaging sensor technology, cameras used in multispectral imaging systems have also been evolved. Many commercial and customized multispectral systems have been developed and used for the different remote sensing applications such as cropland assessment, digital agriculture, and pest management, etc. [120]. Most systems provide 8–16 bit images with 3–12 narrow spectral bands in the visible to near infrared (NIR) region of EM spectrum [60, 218, 222].

Multispectral imaging systems are based on different approaches. One approach employs monochrome charged couple device (CCD) industrial cameras. Each camera in multispectral system uses different band pass filter. It gives advantage of individual adjustment of camera for focus and aperture settings. However, one disadvantage is that multiple band images need to be properly aligned. Another approach uses beam-splitting prism and integrates multiple sensors to achieve the effect of multispectral imagery. One example of such system is CS-MS1920 multispectral 3-CCD camera (Teledyne Optech, Inc., Vaughan, Ontario, Canada). It uses 3 CCD sensors to produce images in 3–5 spectral ranges with EM spectrum range of 400–100 nm. In this approach, band images are aligned mechanically as well as optically.

The four-camera imaging system developed by U.S. Department of Agriculture, Agricultural Research Service (USDA-ARS) consists of four monochrome CCD cameras, PC with frame grabber and image acquisition software [162, 218]. The camera uses spectral range of 400–100 nm and 12-bit data depth. Spectra-View by Airborne Data Systems, Inc. (Redwood Falls, Minnesota USA) can accommodate up to eight different cameras. These cameras can vary in size, format, and wavelength and contain global positioning system/inertia navigation system (GPS/INS) for precise geo-registration of the images. Spectra-View 5WT captures 12-bit images in six (Blue, Green, Red, NIR, MWIR, LIR) spectral bands. A cheap alternative, Agri-View, can be used to capture same green, NIR, and red band as captured by Spectra 5WT.

Tetracam's multispectral imaging systems (Tetracam, Inc., Chatsworth, California, USA) come in two product families: (1) Agricultural Digital Camera (ADC) and (2) Multiple Camera Array. ADC family is equipped with single camera along with fixed filters at red, green, and NIR wavelength. Some ADC systems (ADC Micro, ADC Lite and ADC) captures 8/10- bit images with 2048×1536 pixels while other (ADC Snap) captures 1280×1024 pixels. MCA family contains 4, 6, and 12 cameras synchronized to take 8/10-bit images with 1280×1024 pixels in visible to NIR wavelengths. The family comes is two versions: standard Micro-MCA and Micro-MCA Snap versions. RGB+3 system by Tetracam has four cameras: one RGB and three monochrome cameras. RGB senses three broad visible bands and monochrome senses three narrow bands which are 680, 780, and 800 nm, respectively. Mcaw (Multiple camera array wireless), comes with a Linux computer system, a storage device for computations and six 1280×1024 snap shutter sensors. Each Tetracam's systems has PixelWrench2 software which allows the editing of the images [164, 169].

Teledyne Optech produces RGB color cameras and thermal cameras both as standalone or integrated in the LIDAR (light detection and ranging) system. RGB CS-10000 and CS-LW640 are the examples of Teledyne's RGB and thermal camera, respectively. CS-10000 has a resolution of 10,320 by 7760 pixels and CS-LW640 comes with resolution of 640×480 pixels. Integrated with Orion C LIDAR system, CS-LW640 is a very powerful tool for 3D mapping of thermal features.

FLIR and ITRES Research Ltd. also offers some thermal cameras. FLIR's T600 series cameras come with the resolution of 640×480 pixels and SC8000-series have the resolution of 1024×1024 pixels. TABI-1800 by ITRES research can differentiate temperature difference of 1/10th of a degree.

8.3.1.2 Multispectral Imaging Systems Using Consumer Grade Cameras

Low cost, compact size, data storage, and user-friendliness are some of the advantages that make a consumer grade camera an attractive choice for remote sensing. Consumer grade cameras are mostly equipped with CCD or CMOS sensors, and Bayer color filter mosaic for arranging the RGB color pixel [16, 80, 167]. Various mosaicing algorithms are used to interpolate complete RGB values for each pixel which aligns the three ban images perfectly. Therefore, these cameras have been used frequently by researcher for the agricultural purposes [6, 140, 166].

In remote sensing, images in visible and NIR bands are commonly used especially in vegetation monitoring. NDVI uses spectral information in NIR and red bands. Consumer grade camera uses filters to block UV and infrared light. These filters can be replaced by long-pass infrared filter to convert the consumer grade RGB camera to NIR camera and obtain NIR images. Some companies, e.g., Life Pixel, provide services for conversion of camera. Long-pass filter of 720- and 830-nm are used to replace NIR blocking filter. All three channels can be used to record NIR radiation and any of the three can be used as NIR channel, however, red channel is mostly preferred because of best sensitivity. These NIR-converted cameras are

proved to be simple and cheaper tools for plant monitoring, crop monitoring, and stress detection [123, 217].

A cheaper and user-friendly imaging systems are required to capture geotagged images at varying altitudes on any traditional or agricultural aircrafts at normal airplane speed [222]. Agricultural aircrafts are readily available platform for airborne remote sensing. If equipped with imaging system, they can be used to get aerial imagery for various applications such as monitoring, detecting stress, and analyses of aerial applications usefulness. Aerial imaging and aerial spraying must not be done simultaneously to avoid contamination of camera.

A USDA-ARS single-camera uses Nikon D90 camera (Nikon Inc., Melville, New York, USA) to capture color images of up to 4288 × 2848, geotag the image and is equipped with LCD monitor to view live image. For dual-camera system, it uses another same D90 camera but modified to NIR camera. Giga T Pro II wireless timer remote receiver (Hahnel Industries Ltd) and a transmitter is attached to the camera to start and stop the image capturing. Both cameras can be mounted on the aircraft with little or no modification [210, 219]. USDA-ARS also produces two other systems: one consists of two Canon (Canon USA Inc.) EOS 5D Mark III cameras to capture images up to 5760 × 3840 pixels; other system by USDA-ARS consists of two Nikon D810 cameras to capture images up to 5760 × 3840 pixels. In both of the systems, one camera is used to capture RGB color image and the other is converted NIR camera with 830-nm long-pass filter. Both systems use the same sensor size (36 × 24 mm) and focal length (20 nm). Cost of each system is around 6500 USD [172, 217, 222].

Due to increasing demand of light-weight and cheaper imaging systems, many consumer grade camera systems are being converted to capture B-G-NIR or G-R-NIR images using single sensor. LDP LLC, for example, provides either of the modified cameras or services for modification. Both cameras can also be used simultaneously and images can be aligned to create five band images. However, unlike NIR-converted cameras, these cameras may suffer from light contamination depending on filters and algorithms used for the band separation. Salam [156] and Rabatel et al. [130] converted a standard RGB camera by replacing NIR blocking filter with long-pass filter to obtain NIR and R bands. However, spatial resolution of the image is reduced due to smoothing effect in the process.

8.3.1.3 Hyperspectral Imaging Systems

Hyperspectral imaging system can capture images in tens to hundreds of narrow and spectral bands from visible to thermal spectral regions. The airborne visible/infrared imaging spectrometer (AVIRIS) was the first hyperspectral imaging system developed by Jet Propulsion Laboratory and proposed to NASA in 1983. It consists of a flight system, ground data system, and a calibration system. It captures images in 224 continuous spectral bands under solar spectral region of EM spectrum. Different detectors are used which are separated by four panels of wavelength ranging from 400 to 2500 nm. It provides 12-bit spectral data (AVARIS). The AVARIS system has

been extensively studied and improved over the time to meet the requirements of the scientists for the research and application purposes. Green et al. [73] provide the overview of AVARIS sensor along with its various scientific applications [143, 160].

HyMap is another popular hyperspectral imaging sensor developed by Integrated Spectronics Pty Ltd. (Sydney, Australia). Initially, it was used for mineral exploration with 96 channels in the 550–2500 nm spectral range [35, 151]. Current HyMap uses 128 bands in the spectral range of 450–2500 nm. The system is mounted with 3-axis gyro stabilized platform for reduced image distortion. Sensor can capture up to 512-pixel images with spatial resolution of 3–10 m for agricultural applications [43, 68, 211]. The compact airborne spectrographic image (CASI) was the first programmable hyperspectral sensor first introduced in 1989 by ITRES Research Ltd. It allowed user to collect the data in specific band and bandwidth by programming the sensor. CASI-1500H, a lighter and smarter design, captures 14-bit images at 288 bands in the spectral range of 380–1500 nm. SASI-1000A captures 1000-pixel images at 200 bands in spectral range of 950–2450 nm. MASI-600, first commercial system, is available with 600 pixels and 64 bands in the spectral range of 3–5 μm. TASI-600 is a hyperspectral thermal sensor which captures 600 spatial pixel images and 32 bands in the spectral range of 8–11.5 nm.

Commercial hyperspectral imaging systems have become advanced with improved spatial and spectral resolutions and improve GPS units for position accuracy. Specim's AISA hyperspectral systems (Spectral Imaging Ltd., Oulu, Finland) is available with spectral ranges from 380 nm to 12.3 μm. It covers VNIR, SWIR, and thermal LWIR spectral ranges. Specims ASIA family of hyperspectral systems include: AisaKESTREL 10 (spectral range of 400–1000 nm), AisaKESTREL 16 (spectral range 600–1640 nm), AisaFENIX and AisaFENIX 1K (spectral range of 380–2500 nm), and AisaOWL (spectral range of 7.7–12.3 μm). All systems come with a GPS system for accurate positioning [152].

Headwall Photonics, Inc. (Fitchburg, Massachusetts, USA) manufactures hyperspectral imaging sensors for UV to visible, VNIR, NIR, and SWIR in the spectral range of 250–2500 nm. It also produces VNIR-SWIR sensor with spectral coverage of 400–2500 nm. It can capture 1600-pixel swath image at hundreds of bands. USDA-ARS in College Station, Texas, uses hyperspectral imaging system with VNIR E-Series imaging spectrometer, a GPS/INS unit, and hyperspectral data processing unit. It can capture 16-bit images within 923 spectral bands, 1600-pixels of swath in the wavelength of 380–1000 nm [161].

8.3.2 Future Trends

This section discusses some of the challenges and future directions for remote sensing. First challenge is that growers do not know about the availability of imagery in the fast changing market; they do not know what type of imagery to select and how to order imagery from the archived data for their particular application. Image

providers and different vendors must develop easy instructions for customers and growers to select and order appropriate imagery. Timely acquisition and delivery of the images is also one of the challenges.

Numerous literature exists on processing and conversion of imagery into useful information and map, however, there exists no standard procedure for converting imagery to vegetation index maps, classification and prescription maps. There are many image processing software with different capabilities, complexities, and prices. However, grower may have difficulty in choosing a particular software.

There is a dire need of practical guidelines for the growers and other end users for the conversion of images to appropriate agricultural maps. Researchers need to focus on this area. Users having some familiarity with GIS and image processing must be able to select and use appropriate software with the help of documentation and tutorial. If a grower cannot learn these skills, they can use commercial services to process their images and create the relevant maps. Some dealers do provide services of image acquisition, prescription map creation, and variable rate application.

Environmental changes in agriculture may result in large variations in soil moisture, plant nutrition, crop growth and yields. Fast crop canopy changes need continuous crop monitoring [180]. Remote imagery and satellite imagery have been successfully used in crop prediction. However, coarse spatial and temporal resolution makes their application in agriculture very limited. Airborne multispectral (e.g., [220, 221] and hyperspectral [45] have been used to monitor crop condition and yield.

The recent development in small unmanned aerial systems (UASs) makes agriculture sector a largest commercial market for its use and it will see an increase of 80–90% in market share (Association of Unmanned Vehicle Systems International, 2013). Cost-efficient, ultra-high spatial imagery, and easy image acquisition makes UAS an ideal option for crop monitoring. It is also known by various different names: unmanned aerial vehicles (UAVs), drones, unmanned aircraft systems, and remotely piloted vehicle [122].

Applications of UAS in agriculture include: monitoring of physiological characteristics of crops, leaf area index (LAI), disease and crop stress, monitoring of crop growth [19], yield, removal of rainwater [228], spraying fungicide, herbicide, and pesticide [125, 161], air broadcasting of seeds [106], and measuring of crop and environmental parameters (temperature, humidity, etc., [136]). There remains a security and privacy concern regarding the civilian use of UAS, however, its usefulness has already been established among the public specially in the agricultural sector [66].

8.4 Soil Sensing from the Air

Airborne imaging systems are relatively cheaper, provide high spatial resolution, and have the ability to obtain data in visible to shortwave infrared (SWIR) region of EM spectrum [98, 115, 141]. There are two type of imaging systems: (1)

multispectral and (2) hyperspectral. They differ in spectral bands and bandwidth. Multispectral uses 3–12 and hyperspectral uses tens to hundreds spectral bands to measure the reflected energy. Imagery from hyperspectral has great details of spectral bands and multispectral is great in detecting subtle difference among similar objects. We will discuss in detail the airborne multispectral and hyperspectral imaging systems in coming sections.

UAVs are comprised of two main components: UAVs and sensors. UAVs act as a platform for the sensors. UASs can be classified into two categories: (1) fixed-wing, (2) rotatory-wing [171, 176]. Fixed-wing has long range and is faster, however, ideal takeoff and finding landing spot for them are a challenging task. On contrary, rotatory-wing UASs have short range and flight duration but improved maneuverability. In addition to the sensors, platform may be equipped with the global navigation and satellite system (GNSS) and an inertial management unit (IMU). GNSS provides information about the position of the platform and IMU provides information about the altitude of the platform. This information is integrated with the autopilot system to adjust the course of the flight.

One of the challenges in operating UAS is the restriction put by a country on their operation. Canada, for example, does not allow to fly a UAS more the 90 m of height which gives the images with small footprints. This makes it difficult to map a large crop field especially when the average crop field size was 315 ha in Canada in 2010.

Figure 8.2 shows variety of sensors and cameras are available for UAS. The performance of both, multispectral and commercial, cameras is very good [74, 149]. Although, data quality is a concern for the commercial camera [214], however, its low cost for data acquisition makes it an appealing option for agriculture. Simple RGB camera is not only cost-efficient but also a powerful tool for monitoring plant condition and plant phenology [71]. Consumer grade cameras are sensitive to illumination, hence they either must be used under stable lights or adjustment should be made with variable illumination [131, 142].

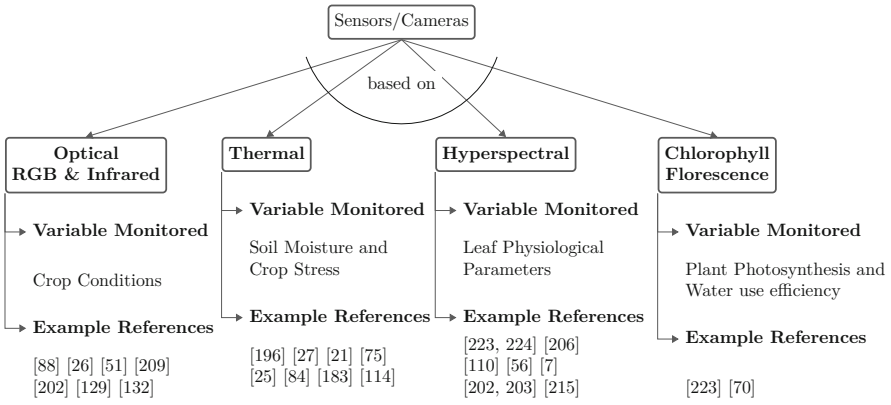

Fig. 8.2 Sensor types and crop monitoring variables [33]

8.4.1 Flight Planning

8.4.1.1 Image Acquisition

Most UASs are using autopilot flight planning for image acquisition. A flight plan includes: area, height course, and speed of the flight, camera setting, forward and side lap; and it is generated using a planning software. Manual control is also possible, however, may cause issues with image post-processing. High-resolution images or high-scale map is shown as a background for the planning and it is stored prior to field trip. GNSS and IMU data are also recorded which assist to determine image center position and camera orientation estimations [163, 188, 214]. All data are initially stored in a storage device in UAS and must be downloaded to the computer for further usage and processing.

The altitude of the flight determines the spatial resolution of images; lower altitude, e.g., 100 and 120 m are common, gives images with the high spatial resolution. For some tasks, e.g., weed mapping, a much lower altitudes (30 m) are also used which results in much higher spatial resolution. However, altitude is also limited by aviation regulations. Flight altitude does not affect VIs, however, it greatly influences the image segmentation with mixed pixels in images with higher altitudes [131, 148]. Four pixels are necessary to identify and find ground object.

Image overlapping is also an important factor to consider for flight planning. Salam [158] and Colomina and Molina [36] suggest to set the minimum value of forward and side overlap to 80% and 60%, respectively. High image overlap is recommended to avoid mismatch between estimated and actual ground image [170, 214], assist in identifying common points in image pair, and minimize the impact of bidirectional reflectance by allowing image processing software to extract the central points of the image for image mosaic [89, 146].

Prior to image acquisition, researchers have used ground control points (GCP), as an artificial target, for spectral calibration. It is recommended to use minimum of three GCPs evenly distributed covering the whole study area [188]. Position of these GCPs should be measured using a total station or differential GNSS to guarantee positional accuracy of image mosaic [47, 157].

8.4.1.2 Image Processing

Various photogrammetry algorithms are used to rectify and mosaic images. After downloading images and logs, initial position and orientation estimates are determined using log files. Ortho-rectified mosaic is generated using various photogrammetric software (e.g., GeoLink [181] and MicMac [13]). Structure from Motion (SfM) photogrammetry has recently become popular for many UAS applications. It uses bundle adjustment algorithms for establishing the structure of the scene, internal and the external orientations [1, 154, 188]. SfM has advantages of having a simple processing workflow, ability to calculate the camera position, orientation,

and scene of the geometry from overlapping images only, not requiring camera calibration parameters and lastly, getting height from two-dimensional images [188]. Pix4Dmapper [131, 155], Agisoft PhotoScan Pro [19], and Automatic Photogrammetric Software are some of the commercially available SfM software. Freely available SfM Web services include Autodesk 123D Catch and Microsoft Photosynth. However, both services were discontinued in 2016 and 2017. Bundler, VisualSFM, Multi-View Stereo (PMVS2), and Ecosynth fall under the category of open-source SfM packages. Although they have been criticized for their computational time and reliability, their performance is sometimes found to be at par with some of the commercially available options [100, 188].

8.4.1.3 UAS Image Applications in Digital Agriculture

Researchers have been using UAS imagery for extracting glut of agricultural data. UAS imagery data includes: plant height, crop biological parameters, and plant stress.

Plant height is a key indicator for predicting many parameters such as: crop biomass and yield potential, growth, treatments and stress monitoring, underlying biophysical, ecological, and hydrological processes [19, 71, 150]. Plant height can be derived from LiDAR or SfM-based photogrammetry. Terrestrial laser scanning (TLS) accurately measures plant height for modeling of crop surface and growth monitoring [185, 197, 199].

Although Direct DEM product of SfM produces a digital surface model, vegetation canopy points can be filtered from point cloud to obtain ground surface elevation point (DTM). Separating ground from non-ground points helps in estimating biomass and other relevant parameters [1, 71, 188]. However, separation of vegetation information has been only partially successful [64, 159]. DTM can also be extracted using UAS before and after growing season [19]. SfM-based heights are found to be more accurate than the TLS-based heights. Moreover, lower altitudes (e.g., 40 m) give more accurate crop heights [86, 153].

Many studies have shown the application of UAS in monitoring crop biological parameters. Information from UAS imaging has been used for evaluation of plant growth, biomass, physiological changes, stresses, and many other crop biological properties. LiDAR, thermal, and hyperspectral sensors are used in this type of research. The biological parameters are highly effected if crop is stressed (water, diseases, and infection from pests, etc.). 20% of irrigated land of the world has high salt concentration [117]. It can cause stomatal closure, decreased photosynthesis, increased leaf temperature [177]. Crop stress can be monitored by the data from periodic thermal and visible to NIR UAS imaging during the growth season.

Thermal UAS imaging can be used to measure temperature for calculating crop water stress index for leaf anomalies [18, 81]. Thermal remote sensing is also used to measure the soil moisture and texture, crop residue cover, field drainage tiles, and yield [96]. Apart from remote sensing, optical sensing can also be used to identify plant conditions. Nutrient deficiencies in plants make them more susceptible to

herbivores pests [168, 177]. Optical UAS images have been used to detect symptoms for plant nutrient deficiencies [34, 183].

Weeds compete with the crops for the natural resources, e.g., solar radiation, nutrition, and water. Site-specific weed management can decrease the cost of crop production and lower the environmental impact. Ultra-high resolution UAS images help in early and late season detection of weed's species, density, and patches [127, 128]. Due to spectral similarities between weeds and crops, hyperspectral sensors are more useful than multispectral sensors [109]. UAS imaging have been used in assessing disease development, atmospheric pathogen development and monitoring, and precision spraying [11, 100, 165]. However, UAS-based sensing for assessment of diseases is still not in the mature stage [144, 147, 177].

8.4.1.4 Image Analysis

Prior to analysis of UAS images, some categorical information, e.g., crop type, lodged crop, stressed crop ,etc., needs to be extracted. Many researchers adopt classification methods while doing qualitative analysis for assigning different class labels. These classification methods can be supervised or unsupervised methods. Some machine learning algorithms are also developed for segmentation of vegetation and bare soil [53].

For quantitative analysis, VIs are computed to find relation between spectral and field biological data [88]. Digital numbers, Vis, and reflectance can be linked to crop biological and environmental parameter. Most common VI, NDVI, is used to measure biomass, nitrogen content, chlorophyll content, and other biological parameters. Soil adjusted VI is used to amplify spectral difference between vegetation and soil [185]. RGB camera-based VIs (Green NDVI, Excess Green Index (ExG), Green Ratio VI) proved to be a good indicator of leaf area, pigment content, and canopy structure [131]. Some VIs are also used to detect vineyard water stress [14, 141, 163]. Studies have indicated that VIs derived from UAS are comparable to those derived from other remote sensing method (e.g., satellite and manned aircraft) and also provide more spatial details.

8.4.2 Future Trends and Conclusion

UAS has become very popular option for monitoring of crops' biological and environmental parameters, however, they are relatively expensive option. There exists no straightforward procedure for image interpretation, processing, and analyses and it requires considerable amount of expertise and skilled technicians to use this option [13]. A straightforward and an automated tool should be developed for wider adoption of UAS in agriculture [185]. UAS may not be able to cover large enough area which can cause technical difficulties. Furthermore, advancement and development of UAS technology also rely on loosening of aviation regulations.

Local producers must be educated on what cost-effective UAS options are available to them. Due to involvement of different equipment's and requiring high technical expertise from different area, a group of researcher can be formed to raise awareness among farmers on using these systems [185, 227]. Farmers, either as a group or individually, can also hire the consultancy service to receive proper guidance [227].

8.4.3 NASA Soil Moisture Active Passive Mission

NASA sent a Soil Moisture Active Passive (SMAP) satellite for research purpose carrying an L-band radiometer (resolution = 40 km) on January 31, 2015. This satellite was capable of detecting passive microwave radiation emitted by the Earth. It was also equipped with the radar (resolution ≈3 km) for sending microwave to the surface of the earth and detecting the reflection. The mission was to measure soil moisture and detect water freeze/thaw states. Backscatters from radars were affected by the vegetation, bodies of water, and surface irregularities. Therefore, signals from radiometers and radars were combined to get soil moisture reading within 9 km resolution [58, 197]. The radar amplifier was failed on September 2, 2015, because of which it stopped working. However, NASA was successful in getting images of 20 km resolution by using different methods such as interpolating and de-convolution and also the oversampling of radiometer. Another approach can read image of 1 km resolution by applying active-pass algorithm to the images from other radars [126, 162]. The mission's data plays an important role in developing weather, soil moisture model, and carbon cycle but SMAP accuracy is major concern.

8.4.3.1 Cosmic-Ray Neutron Probes

A neutron probe is an amalgamation of beryllium and a radioactive material which releases high- and low-speed neutrons. High-speed neutron collides with light hydrogen atom to produce a high amount of energy, whereas low-speed neutron forms a cloud whose density is directly proportional to the soil–water content, e.g., dry soil will create a less dense cloud, fewer low-speed neutron, and less amount of water [134]. Cosmic-ray neutron probes (CRNP) work on the same principle. High-speed neutrons are produced by cosmic rays coming from space and can reach several hundred meters. Soil moisture is inversely proportional to the effective depth. However, while calibrating the instruments, it is very important to consider the other hydrogen sources, e.g., decomposing soil organic component and humus, and need average in-situ soil moisture measurement and neutron intensity [124]. It is also important to properly follow security and safety infrastructure to avoid any radiation hazard while CRNP [17, 30].

Franz et al. [65] did a comparative investigation for soil–water content (SWC) readings taken by in-situ time-domain transmissivity (TDT) sensors and CRNP. The mean absolute error of 0.0286 m^3/m^3 was measured. However, while taking SWC

measurement from TDT sensors, the sensors were not permanently installed in the field due to their sparse distribution. Similarly, readings from CRNP do not include vegetation type.

8.4.3.2 GPS Interferometric Reflectometry

Global positioning system (GPS) also uses L-band microwaves. GPS interferometric reflectometry can detect conditions like snow depth, soil moisture, and vegetation water content. To does so by detecting the temporal changes in SNR of line-of-sight (direct wave) and multipath reflected component [31, 172]. Soil permittivity affects the reflected wave and can change frequency, phase, and amplitude of the signal. These signal snapshots are referred to as interferograms. Geodetic-quality GPS antennas can detect soil moisture from a very small distance (2–5 cm) from the surface. It is fixed on airborne devices. However, one disadvantage of the scheme is that it highly dependent on constellation of GPS satellites. These satellites move around the earth few times a day, hence limiting the number of estimations [124, 168].

8.4.3.3 Wireless Sensor Networks

Precision irrigation applications require high spatio-temporal resolution for proper working which is provided by the sensor networks. Wireless communication helps in providing remote information access. This information is provided in real-time so that manual manipulation can be avoided to get an idea about the field conditions. Dong and Vuran [49] used small amount of sensors for measuring soil moisture because of precipitation duration and rainfall cell radius magnitude.

Vereecken et al. [207] discuss various techniques for estimating exact location of the sensor nodes. In general, examining different soil properties with varying soil moisture level can give an average soil moisture value for the field. Delgado and Martínez [44] calculate location-specific solar radiation intensity values to estimate the evaporation rate corresponding to that certain location. A mobile application is used for this approach. The calculations matched the reading from agriculture station which helped in generalizing the result to all those locations which have same radiation conditions. Sensor cluster is then placed in chosen area with following the recommendations given in [49, 164, 169].

The primary task in the WUSN is to determine number of sample readings. It is important because sensing and communicating data consumes large amount of power [49, 166]. Shallow roots and high porosity cause speedy water infiltration and evaporation in soil. Therefore, large sampling rate is needed to overcome this highly fluctuating effect.

8.5 Soil Moisture Sensors Calibration

Extensive research is being done in designing efficient and accurate soil moisture sensors for the irrigation applications [40, 62, 91, 101, 129, 139, 142, 229]. The aim is to avoid financial losses because of over- and under-irrigation. The studies help in (1) selecting accurate soil moisture sensor based on the soil texture, (2) error rate of the sensor, and (3) using calibration method that can help in accurate decision making. The adoption rate of sensing technologies has been very slow not only in America but globally as well. For example, in the United States, Nebraska leads the sensors adoption rate by 30.5% in 2013 [204]. Nebraska has taken a firm position in agricultural water management. The organizations like Nebraska Agricultural Water management (NAWMN) [92] spread the farm-level technologies among 1500 collaborators to increase the adoption rate among stakeholders, i.e., producers, advisors, and crop consultants, etc. However, there is still need to improve the agricultural use and management of water given the fact that on 11.2% of the United States farms use soil moisture based sensor devices [171, 204].

About 90% of farms in the United States do not adopt science-based irrigation water management technologies which raises the questions about the effectiveness of ongoing research. The major challenge in soil moisture adoption rate is the lack of well-defined guidelines to train users to understand and what to expect of technology. When one has to choose from multitude of available sensors, it can cause uncertainty due to different soil textures, therefore, suitability is an important aspect to look for while increasing the adoption rate. In addition to accuracy, operational feasibility, e.g., financial, ease of operation, durability and logistic features of a sensor are also very important. Although, accuracy is the primary concern for scientific users, however, operational feasibility plays an important role in changing preferences of commercial in selecting sensors. For example, a field with high spatial variability will require many sensors in to cover multiple sites and labor to deploy those sensors. Therefore, operational feasibility parameters (time, cost, and labor) will be important inputs to consider, in addition to accuracy, while implementing the system [150, 160].

In coming sections, a framework is provided to evaluate the sensors on the basis of accuracy and operational feasibility. A total of nine commercially available sensors are used along with the two different soil types: Silt loam and sandy soil. Two different orientations of sensing equipment, i.e., horizontal and vertical to ground surface, are used. Finally a decision-making guide is presented to help selecting the sensors on the basis of accuracy and operational feasibility [144, 149].

8.5.1 Materials and Methods

- ***Experimental Sites***: Outdoor field experiments were conducted in two sites with each having different soil types (sandy and silt loam) in Nebraska during growing

Table 8.2 Experiment site details [101]

Site features	Site 1	Site 2
Location	University of Nebraska-Lincoln South Central Agricultural Laboratory (SCAL), near clay center, Nebraska	Central City approximately 10 km north of the Platte River, Nebraska
Average annual precipitation	730 mm	732 mm
Average growing season precipitation	437 mm	464 mm
Soil type	Well-drained Hastings silt loam soil	Deep, moderately drained, and moderately permeable loamy sand
Soil field capacity (FC)	0.34 $m^3\ m^{-3}$	0.19 $m^3\ m^{-3}$
Soil permanent wilting point (PWP)	0.14 $m^3\ m^{-3}$	0.05 $m^3\ m^{-3}$
Crops grown	Field maize and Soybean	Buffalo grass and tall fescue
Size of the field	16.5 ha	70 ha

season of 2017 and 2018. Rest of the discussion will refer these sites as per the soil type, i.e., sandy and silt loam. These two soil types provide an opportunity for sensor evaluation in irrigated and rainfed agricultural systems. Table 8.2 lists the important details pertaining to both experimental sites.

- ***Sensors***: As discussed earlier, a total of nine sensors. These nine sensors were evaluated in two sets of each sensor: horizontal orientation and vertical orientation. The only exceptions were JD multi-sensor probe and TDR315L (Acclima) because that can only be used vertically and horizontally, respectively. Following sensors were used for the experimentation [20, 46, 52, 67, 72, 110, 114, 182, 194, 200, 201, 205, 208, 215, 224, 225]:
  - TrueTDR-315L (Acclima, Inc., Meridian, ID)
  - CS616 (Campbell Scientific, Inc., Logan, UT)
  - CS655 (Campbell Scientific, Inc., Logan, UT)
  - 5TE (Meter Group, Pullman, WA)
  - SM150 (Delta-T Devices, Cambridge, U.K.)
  - 10HS (Meter Group, Pullman, WA)
  - John Deere (JD) Field Connect (John Deere Water, San Marcos, Cal.)
  - EC-5 (Meter Group, Pullman, WA)
  - Dielectric Water Potential-based SensorTEROS 21 (MPS-6) (Meter Group, Pullman, WA)

  The first three are time-domain reflectometry (TDR)-based sensors and others are capacitance-based sensors. The sensors measure volumetric water content (θ_v) ($m^3\ m^{-3}$%vol) except TEROS 21 (MPS-6), which gives soil matrix potential (Ψ_m) (kPa) and is converted to θ_v by soil-specific soil–water release curves given by.

- ***Reference (True) Moisture Measurement*:** Reference soil moisture values θ_v (θ_{vref}) have been measured using Troxler Model 4302 neutron probe (NP) soil moisture gauge (Troxler Electronic Laboratories, Inc., Research Triangle Park, N.C.). All other sensor values are calibrated on the basis of NP measurements. Factory calibrated NP measurement is correlated with gravimetric-sample determined θ_v to develop site-specific calibration using following equations:

$$y = 0.9061x + 0.0354 \tag{8.2}$$

$$y = 1.0848x - 0.0246, \tag{8.3}$$

  where y is θ_{vref}, x is θ_v and Eq. (8.2) and (8.3) are measures calibration for silt loam and sandy soil, respectively.
- ***Installation Specifications*:** Sensor output accuracy is also dependent upon how they are installed in the field. Four soil type-orientations were referred as: silt loam H, silt loam V, loamy sand H, and loamy sand V, where H and V represent the vertical and horizontal orientation. For horizontal orientation (silt loam H, loamy sand H): soil pits were dug on both sides of sensors in furrow (silt loam soil) and grassed area (loamy sand soil). Sensors were installed parallel and perpendicular for horizontal and vertical orientation, respectively. The distance between the sensors is kept such that one sensor may not affect the readings from other sensor. For vertical orientation, distance between the horizontal plane and the ground surface is kept 30 and 50 cm for silt loam and loamy sand soil, respectively. The JD probe uses different orientation because of its distinguishing characteristic of being a multi-depth probe and is compared with NP probe at multiple depths (10, 20, 30, 50, and 100 cm).
- ***Soil Moisture Data Measurement and Retrieval*:** Dataloggers are used to collect data from the sensors about soil moisture every minute and hourly averages. Only in the case of JD probes, telemetry was used to collect data. NP measurements were taken every week throughout growing season.
- ***Statistical Analysis***: For performance evaluation of sensors, root mean squared error (RMSE, $m^3\,m^{-3}$) is computed as follows:

$$\text{RMSE} = \sqrt{\frac{\sum_{i=1}^{n}(E_i - M_i)^2}{n}}, \tag{8.4}$$

  where n is total number of observations, M_i is sensor values, and E_i are corresponding NP-probe measure values. RMSE value is used as absolute value of error for a particular sensor.
- ***Evaluation Metrics***: The two metrics used for the each sensor evaluation are: Operational feasibility and performance accuracy. The next two sections briefly explain how sensors are evaluated for these metrics.

8.5.2 Operational Feasibility

Operational feasibility of a sensors can be expressed by the following four characteristics:

- *Telemetry.* Telemetry (TM) refers to real-time access of soil moisture data from the site on mobile or web platforms which is transmitted using some terrestrial or radio system. It prevents users from labor and time investment of going physically to the site and monitoring water profile of the soil [157]. The TM information is quantified by following equation and referred to as $Score_1$:

$$Score_1 = \begin{cases} 0 & \text{No TM} \\ 100 & \text{With TM} \end{cases} \tag{8.5}$$

- *Sensor Cost.* Sensor cost plays a very important role in selection of sensor. The absolute cost of sensor (Table 8.3) is quantified and rescaled to scale of 0–100 to be consistent with other factors scores and is represented by $Score_2$ as follows:

$$Score_2 = 100 - \left(\frac{Max_{scaled} - Min_{scaled}}{Max_{cost} - Min_{cost}} \right) \times (Sensorcost - Min_{cost}) + Min_{scaled}, \tag{8.6}$$

  where Max_{scaled} and Min_{scaled} are extremes of score metric (0 and 100), and Max_{cost} and Min_{cost} are extremes of absolute cost of sensors in USD. Cheapest sensor will have the score of 100 and expensive sensor will have score of 0.
- *Cost of Sensing and DataLogging.* Accurate sensing and datalogging after fixed intervals (e.g., 30–60 min) is an important part of sensor operations. It gives daily status as well as the historical soil moisture data for decision making and scrutiny of data for quality purposes. Therefore, Eq. (8.7) and (8.8) give the total cost of sensing and datalogging with and without TM, respectively:

$$\text{Total Cost}_{NoTM} = \text{Sensor Cost} + \text{DL cost} \tag{8.7}$$

$$\text{Total Cost}_{TM} = \text{Per sensor cost} + \text{DL cost} + \text{TM cost} \tag{8.8}$$

  The total cost of the sensor (Table 8.3) is quantified and rescaled as $Score_3$ using method similar to used in $Score_2$ computation as follows:

$$Score_3 = 100 - \left(\frac{Max_{scaled} - Min_{scaled}}{Max_{Totalcost} - Min_{Totalcost}} \right) \times (Totalcost - Min_{Totalcost}) + Min_{scaled}, \tag{8.9}$$

Table 8.3 Prices (in USD) of sensors and corresponding dataloggers as on March 2019 [101]

Sensor	Sensor cost ($)	Sensing and logging cost ($) (No TM)	Sensing and logging cost ($) (TM)
CS655	228	1928	2378
CS616	148	1848	2298
SM150	230	1590	3590
10HS	128	624	1274
EC-5	120	616	1266
5TE	225	721	1371
TEROS 21 (MPS-6)	225	721	1371
JD Probe	193	1193	2193
TDR315L (Acclima)	295	670	N/A (not available from manufacturer)

where Max_{scaled} and Min_{scaled} are extremes of score metric (0 and 100), and $Max_{Totalcost}$ and $Min_{Totalcost}$ are the extremes of absolute total cost of sensors in USD (Table 8.3). Cheapest sensor will have the score of 100 and expensive sensor will have score of 0.

- *Ease of Operation.* Ease of operation can be assessed by measuring ease of interaction with users at various stages. The stages can be categorized to setting up datalogger, collecting data from datalogger and post-processing the data. The following $Score_4$ for this factor is quantified based on the factor if in a sensor datalogger comes with a graphical user interface (GUI) and if post-processing of data is needed for the sensor:

$$Score_4 = \begin{cases} 0 & \text{No GUI} \\ 100 & \text{GUI, no data post-processing} \\ 50 & \text{GUI, require data post-processing} \\ 1 & \end{cases} \tag{8.10}$$

All scores apply to any orientation and soil type and remain unchanged if site-specific calibrations (S.S.C.) or factory calibrations (F.C.) are used.

8.5.3 Performance Accuracy

The performance accuracy shows the ability of sensor to accurately sense the data. It is dependent upon soil type and orientation, therefore, for all soil type and orientation combinations, root mean squared error (RMSE), for each sensor's θ_v, is measured against reference values from neutron probes. To be consistent with operational feasibility, RMSE values are scaled to have score of 0–100 referred as a performance accuracy (P.A.) score. P.A. score is computed as follows:

Table 8.4 Root mean squared error RMSE ($m^3\ m^{-3}$) for each sensor using multiple orientations, soil types, and calibration types [101]

Soil type	Sensor	RMSE ($m^3\ m^{-3}$)			
		Vertical		Horizontal	
		F.C.	S.S.C.	F.C.	S.S.C.
Silt loam	CS655	0.05	0.03	0.15	0.05
	CS616	0.06	0.03	0.40	0.05
	SM150	0.0	7 0.02	0.06	0.04
	10HS	0.10	0.03	0.07	0.06
	EC-5	0.15	0.03	0.15	N/A
	5TE	0.05	0.02	0.06	0.04
	TEROS 21 (MPS-6)	0.08	0.03	0.11	0.05
	JD Probe	0.05	0.06	N/A	N/A
	TDR315L (Acclima)	N/A	N/A	0.06	0.04
Loamy sand	CS655	0.03	0.03	0.01	0.02
	CS616	0.03	0.02	0.03	0.025
	SM150	0.04	0.04	0.02	0.02
	10HS	0.04	0.02	0.14	0.02
	EC-5	0.05	0.04	0.09	0.02
	5TE	0.04	0.04	0.03	0.01
	TEROS 21 (MPS-6)	0.21	0.03	0.22	N/A
	JD Probe	0.01	0.02	N/A	N/A
	TDR315L (Acclima)	N/A	N/A	0.02	0.02

$$P.A.score = 100 - \left(\frac{Max_{scaled} - Min_{scaled}}{Max_{RMSE} - Min_{RMSE}}\right) \times (RMSE - Min_{RMSE}) + Min_{scaled}, \tag{8.11}$$

where Max_{scaled} and Min_{scaled} are extremes of score metric (0 and 100), and Max_{RMSE} and Min_{RMSE} are the extremes of sensor's RMSE value (Table 8.4). Most accurate sensor will have the score of 100 and least accurate sensor will have score of 0.

8.5.4 Results and Discussion

Scores from Eqs. (8.5), (8.6), (8.9), and (8.10) were used to assess operational feasibility of a sensor (see Table 8.5). All sensors, except TDR-315L (Acclima), were scored 100 for $Score_1$. TDR-315L (Acclima) was scored 0 because of non-availability of TM. $Score_2$ shows more variability than $Score_1$ with EC-5 having lowest score of 0 (most expensive) and TDR-315L (Acclima) sensors having the maximum score of 100 (cheapest). Rest of the sensors did not had much difference

Table 8.5 Total score calculated for each sensor for operational feasibility (O.F.) and performance accuracy (P.A.)

Operational feasibility (O.F.) score					
Column ID	1	2	3	4	5
Sensor	Score 1	Score 2	Score 3 (non-TM)	Score 3 (TM)	Score 4
CS655	100	38	0	52	0
CS616	100	84	6	56	0
SM150	100	37	26	0	100
10HS	100	95	99	100	100
EC-5	100	100	100	100	100
5TE	100	40	92	95	100
TEROS 21 (MPS-6)	100	40	92	95	50
JD Probe	100	58	N/A	60	100
TDR315L (Acclima)	0	0	96	N/A	100

Performance accuracy (P.A.) score							
6							
Silt loam V		Silt loam H		Loamy sand V		Loamy sand H	
F.C.	S.S.C.	F.C.	S.S.C.	F.C.	S.S.C.	F.C.	S.S.C.
100	76	73	47	90	66	100	53
87	80	0	31	94	74	95	79
74	100	100	80	85	0	98	0
44	84	95	2	87	100	41	8
0	75	73	N/A	84	17	65	84
97	94	100	100	87	11	91	100
67	80	85	72	0	23	0	N/A
99	0	N/A	N/A	100	81	N/A	N/A
N/A	N/A	98	83	N/A	N/A	97	8

P.A. scores may differ from parameters of experiments, e.g., soil types, orientations, and calibration whereas scores for O.F. are universal [101]

($225–$230) with the scores ranging between 37 and 40. For $Score_3$, there can be two cost cases: with or without TM. In category of sensors without TM sensing and datalogging, EC-5 and CS655 were the cheapest and the most expensive sensors, respectively. In category of sensors with TM sensing and datalogging, EC-5 and SM150 were the cheapest and the most expensive sensors, respectively. TM options had a significant impact on the total cost of the sensor, hence, also on the selection of sensor. Finally, all sensors, except CS616, CS655, and TEROS 21 (MPS-6), score 100 in $Score_4$. Because of need of programming for setting up the datalogger for CS616 and CS655, they were scored 0 for $Score_4$. Similarly, TEROS 21 required data post-processing and was scored 50 for $Score_4$ [149, 152].

P.A. scores were calculated for four soil type and orientation combinations: silt loam H, silt loam V, loamy sand H, and loamy sand V, using Eq. (8.11) (see

Table 8.5). P.A. scores are studied from the three perspective: on the basis of site, calibration type, and orientation. For silt loam V, CS655 with highest P.A., and EC-5 with lowest P.A., had extreme P.A. score values under F.C., and SM150 with highest P.A., and JD Probe with lowest P.A., had extreme P.A. score values under S.S.C. It is interesting to note that changing the calibration method completely alters the P.A. scores. For silt loam H, 5TE SM150 with highest P.A., and CS616 with lowest P.A. had extreme P.A. score values under F.C., and 5TE with highest P.A., and 10 HS with lowest P.A., had extreme P.A. score values under S.S.C. It is interesting to note that 5TE performed well in all conditions and can be a suitable choice for irrigation applications. For the soil type, following changes were observed for P.A. scores: 10 HS (loamy sand V under S.S.C.), JD probe (for loamy sand V under F.C.), CS655 (loamy sand H under F.C.), and 5TE (loamy sand H under S.S.C.). P.A scores are singular for the sensors and do not have constituent as in operational feasibility scores and it is significantly affected by changing the orientation, soil type, and calibration type [100, 165, 210, 211].

8.6 A Guide for Sensor Selection

Figure 8.3 gives a step-by-step sensor selection framework to help choosing appropriate sensors for given conditions. The steps of this framework are as follows:

- Choose appropriate factors among operational feasibility components and P.A which are most relevant to the users condition to recognize the sensors with characteristics more closer to user demand, e.g., for a highly skilled research ease of operation ($Score_4$) can be ignored.
- Each factor is assigned a weight on the basis of importance to user, e.g., for research purpose P.A. scores are assigned high weight.
- The assigned weight is multiplied with the corresponding score of the factor. As an example, an equation is shown in Fig. 8.3-step 3 where various individual

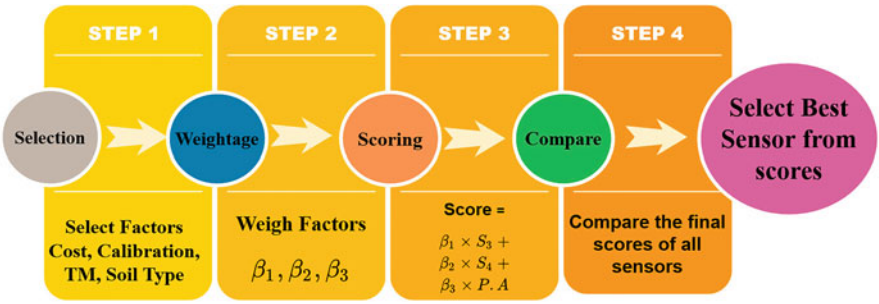

Fig. 8.3 Selection procedure of soil moisture sensors

factors scores for ease of operation, sensing and datalogging cost, and P.A. scores are multiplied by corresponding weights (β_2, β_1, β_3), respectively, and a final score is computed.
- All sensors are compared for the final scores for evaluation on the basis of degree of success and operational feasibility that can be achieved by a particular sensor. The sensor with the highest final score will be most suited for the application.

References

1. Aasen H, Burkart A, Bolten A, Bareth G (2015) Generating 3d hyperspectral information with lightweight UAV snapshot cameras for vegetation monitoring: from camera calibration to quality assurance. ISPRS J Photogramm Remote Sens 108:245–259
2. Abendroth L, Elmore R, Boyer M, Marlay S (2011) Corn growth and development. pmr 1009
3. Adamchuk VI, Hempleman CR, Jahraus DG (2005) On-the-go capacitance sensing of soil water content. In: Mid-central conference. American Society of Agricultural and Biological Engineers, St. Joseph, p 1
4. Adamchuk VI, Rossel RAV, Marx DB, Samal AK (2011) Using targeted sampling to process multivariate soil sensing data. Geoderma 163(1-2):63–73
5. Adamchuk VI, Rossel RV, Sudduth KA, Lammers PS (2011) Sensor fusion for precision agriculture. Sensor fusion-foundation and applications. InTech, Rijeka, pp 27–40
6. Akkaynak D, Treibitz T, Xiao B, Gürkan UA, Allen JJ, Demirci U, Hanlon RT (2014) Use of commercial off-the-shelf digital cameras for scientific data acquisition and scene-specific color calibration. JOSA A 31(2):312–321
7. Allred B, Daniels JJ, Ehsani MR (2008) Handbook of agricultural geophysics. CRC Press, Boca Raton
8. Andrade-Sánchez P, Upadhyaya SK, Jenkins BM (2007) Development, construction, and field evaluation of a soil compaction profile sensor. Trans ASABE 50(3):719–725
9. Antonucci F, Pallottino F, Costa C, Rimatori V, Giorgi S, Papetti P, Menesatti P (2011) Development of a rapid soil water content detection technique using active infrared thermal methods for in-field applications. Sensors 11(11):10114–10128
10. Araus JL, Cairns JE (2014) Field high-throughput phenotyping: the new crop breeding frontier. Trends Plant Sci 19(1):52–61
11. Aylor DE, Schmale DG III, Shields EJ, Newcomb M, Nappo CJ (2011) Tracking the potato late blight pathogen in the atmosphere using unmanned aerial vehicles and Lagrangian modeling. Agric For Meteorol 151(2):251–260
12. Babaeian E, Sadeghi M, Jones SB, Montzka C, Vereecken H, Tuller M (2019) Ground, proximal, and satellite remote sensing of soil moisture. Rev Geophys 57(2):530–616
13. Ballesteros R, Ortega J, Hernández D, Moreno M (2014) Applications of georeferenced high-resolution images obtained with unmanned aerial vehicles. part I: description of image acquisition and processing. Precis Agric 15(6):579–592
14. Baluja J, Diago MP, Balda P, Zorer R, Meggio F, Morales F, Tardaguila J (2012) Assessment of vineyard water status variability by thermal and multispectral imagery using an unmanned aerial vehicle (UAV). Irrig Sci 30(6):511–522
15. Barrios MDR, Marques J Jr, Matias SSR, Panosso AR, Siqueira DS, Scala N Jr (2017) Magnetic susceptibility as indicator of soil quality in sugarcane fields. Revista Caatinga 30(2):287–295
16. Bayer BE (1976) Color imaging array. US Patent 3,971,065
17. Bell J (1987) Neutron probe practice. Institute of Hydrology, Wallingford
18. Bellvert J, Zarco-Tejada PJ, Girona J, Fereres E (2014) Mapping crop water stress index in a 'pinot-noir'vineyard: comparing ground measurements with thermal remote sensing imagery from an unmanned aerial vehicle. Precis Agric 15(4):361–376

19. Bendig J, Bolten A, Bennertz S, Broscheit J, Eichfuss S, Bareth G (2014) Estimating biomass of barley using crop surface models (CSMS) derived from UAV-based RGB imaging. Remote Sens 6(11):10395–10412
20. Berni J, Zarco-Tejada P, Suárez L, González-Dugo V, Fereres E (2009) Remote sensing of vegetation from UAV platforms using lightweight multispectral and thermal imaging sensors. Int Arch Photogramm Remote Sens Spatial Inform Sci 38(6):6
21. Berntsen J, Thomsen A, Schelde K, Hansen O, Knudsen L, Broge N, Hougaard H, Hørfarter R (2006) Algorithms for sensor-based redistribution of nitrogen fertilizer in winter wheat. Precis Agric 7(2):65–83
22. Blackmer T, Schepers J (1995) Use of a chlorophyll meter to monitor nitrogen status and schedule fertigation for corn. J Prod Agric 8(1):56–60
23. Boon N, Yahya A, Kheiralla A, Wee B, Gew S (2005) A tractor-mounted, automated soil penetrometer–shearometer unit for mapping soil mechanical properties. Biosyst Eng 90(4):381–396
24. Bravo C, Moshou D, Orberti R, West J, McCartney A, Bodria L, Ramon H (2004) Foliar disease detection in the field using optical sensor fusion. Agric Eng Int CIGR J, 1–14
25. Breda NJ (2003) Ground-based measurements of leaf area index: a review of methods, instruments and current controversies. J Exp Bot 54(392):2403–2417
26. Bronson KF, White JW, Conley MM, Hunsaker DJ, Thorp KR, French AN, Mackey BE, Holland KH (2017) Active optical sensors in irrigated durum wheat: nitrogen and water effects. Agron J 109(3):1060–1071
27. Bundy LG, Andraski TW (2004) Diagnostic tests for site-specific nitrogen recommendations for winter wheat. Agron J 96(3):608–614
28. Busemeyer L, Mentrup D, Möller K, Wunder E, Alheit K, Hahn V, Maurer HP, Reif JC, Würschum T, Müller J et al (2013) BreedVision—a multi-sensor platform for non-destructive field-based phenotyping in plant breeding. Sensors 13(3):2830–2847
29. Campbell G, Calissendorff C, Williams J (1991) Probe for measuring soil specific heat using a heat-pulse method. Soil Sci Soc Am J 55(1):291–293
30. Chanasyk D, Naeth MA (1996) Field measurement of soil moisture using neutron probes. Can J Soil Sci 76(3):317–323
31. Chew C, Small EE, Larson KM (2016) An algorithm for soil moisture estimation using GPS-interferometric reflectometry for bare and vegetated soil. GPS Solut 20(3):525–537
32. Chrisman BB, Zreda M (2013) Quantifying mesoscale soil moisture with the cosmic-ray rover. Hydrol Earth Syst Sci 17:5097–5108
33. Chunhua Zhang DW, Kovacs JM (2019) The use of unmanned aerial systems (UASs) in precision agriculture, chap 4. Burleigh Dodds Science Publishing, Cambridge, pp 107–128
34. Cilia C, Panigada C, Rossini M, Meroni M, Busetto L, Amaducci S, Boschetti M, Picchi V, Colombo R (2014) Nitrogen status assessment for variable rate fertilization in maize through hyperspectral imagery. Remote Sens 6(7):6549–6565
35. Cocks T, Jenssen R, Stewart A, Wilson I, Shields T (1998) The HyMapTM airborne hyperspectral sensor: the system, calibration and performance. In: Proceedings of the 1st EARSeL workshop on imaging spectroscopy, EARSeL, pp 37–42
36. Colomina I, Molina P (2014) Unmanned aerial systems for photogrammetry and remote sensing: a review. ISPRS J Photogramm Remote Sens 92:79–97
37. Corwin DL (2008) Past, present, and future trends in soil electrical conductivity measurements using geophysical methods. Handbook of agricultural geophysics. CRC Press, Taylor & Francis, Boca Raton, pp 17–44
38. Dash J, Curran P (2004) The MERIS terrestrial chlorophyll index. Int J Rem Sens 25(23):257
39. Datt B (1999) A new reflectance index for remote sensing of chlorophyll content in higher plants: tests using eucalyptus leaves. J Plant Physiol 154(1):30–36
40. Datta S, Taghvaeian S, Ochsner TE, Moriasi D, Gowda P, Steiner JL (2018) Performance assessment of five different soil moisture sensors under irrigated field conditions in Oklahoma. Sensors 18(11):3786

41. De Gruijter J, Brus DJ, Bierkens MF, Knotters M (2006) Sampling for natural resource monitoring. Springer Science & Business Media, Berlin
42. de Souza EG, Scharf PC, Sudduth KA (2010) Sun position and cloud effects on reflectance and vegetation indices of corn. Agron J 102(2):734–744
43. Dehaan R, Taylor G (2002) Field-derived spectra of salinized soils and vegetation as indicators of irrigation-induced soil salinization. Remote Sens Environ 80(3):406–417
44. Delgado B, Martínez M (2015) Software application for calculating solar radiation and equivalent evaporation in mobile devices. Agric Water Manag 151:30–36
45. DeTar WR, Chesson JH, Penner JV, Ojala JC (2008) Detection of soil properties with airborne hyperspectral measurements of bare fields. Trans ASABE 51(2):463–470
46. Diaz-Varela RA, Zarco-Tejada PJ, Angileri V, Loudjani P (2014) Automatic identification of agricultural terraces through object-oriented analysis of very high resolution DSMs and multispectral imagery obtained from an unmanned aerial vehicle. J Environ Manag 134:117–126
47. d'Oleire Oltmanns S, Marzolff I, Peter KD, Ries JB (2012) Unmanned aerial vehicle (UAV) for monitoring soil erosion in Morocco. Remote Sens 4(11):3390–3416
48. Domsch H, Ehlert D, Giebel A, Witzke K, Boess J (2006) Evaluation of the soil penetration resistance along a transect to determine the loosening depth. Precis Agric 7(5):309–326
49. Dong X, Vuran MC (2010) Spatio-temporal soil moisture measurement with wireless underground sensor networks. In: 2010 The 9th IFIP Annual Mediterranean ad hoc networking workshop (Med-Hoc-Net). IEEE, Piscataway, pp 1–8
50. Drummond P, Christy C, Lund E et al (2000) Using an automated penetrometer and soil EC probe to characterize the rooting zone. In: Proceedings of the 5th international conference on precision agriculture, Bloomington, Minnesota, 16–19 July 2000. American Society of Agronomy, Madison, pp 1–9
51. Dualex (2020). https://www.force-a.com/fr/produits/dualex
52. Duan Z, Zhou Q (2015) CRLB-weighted intersection method for target localization using AOA measurements. In: 2015 IEEE international conference on computational intelligence and virtual environments for measurement systems and applications (CIVEMSA). IEEE, Piscataway, pp 1–6
53. Duan T, Zheng B, Guo W, Ninomiya S, Guo Y, Chapman SC (2017) Comparison of ground cover estimates from experiment plots in cotton, sorghum and sugarcane based on images and ortho-mosaics captured by UAV. Funct Plant Biol 44(1):169–183
54. Durner W, Germer K, Jackisch C, Andrä I, Schulz K, Schiedung M, Haller-Jans J, Schneider J, Jaquemotte J, Helmer P et al (2020) Feldstudie zur bodenfeuchtesensorik
55. Dworak V, Selbeck J, Ehlert D (2011) Ranging sensors for vehicle-based measurement of crop stand and orchard parameters: a review. Trans ASABE 54(4):1497–1510
56. Ehlert D, Dammer KH (2006) Widescale testing of the crop-meter for site-specific farming. Precis Agric 7(2):101–115
57. El-Shikha DM, Barnes EM, Clarke TR, Hunsaker DJ, Haberland JA, Pinter P Jr, Waller PM, Thompson TL (2008) Remote sensing of cotton nitrogen status using the canopy chlorophyll content index (CCCI). Trans ASABE 51(1):73–82
58. Entekhabi D, Njoku EG, O'Neill PE, Kellogg KH, Crow WT, Edelstein WN, Entin JK, Goodman SD, Jackson TJ, Johnson J et al (2010) The soil moisture active passive (SMAP) mission. Proc IEEE 98(5):704–716. https://doi.org/10.1109/jproc.2010.2043918
59. Erdi-Krausz G, Matolin M, Minty B, Nicolet J, Reford W, Schetselaar E (2003) Guidelines for radioelement mapping using gamma ray spectrometry data: also as open access e-book. International Atomic Energy Agency (IAEA), Vienna
60. Everitt J, Escobar D, Cavazos I, Noriega J, Davis M (1995) A three-camera multispectral digital video imaging system. Remote Sens Environ 54(3):333–337
61. Evett S, Parkin G (2005) Advances in soil water content sensing. Vadose Zone J 4(4):986–991
62. Evett S, Steiner J (1995) Precision of neutron scattering and capacitance type soil water content gauges from field calibration. Soil Sci Soc Am J 59(4):961–968

63. Feng W, Shen W, He L, Duan J, Guo B, Li Y, Wang C, Guo T (2016) Improved remote sensing detection of wheat powdery mildew using dual-green vegetation indices. Precis Agric 17(5):608–627
64. Fernández T, Pérez JL, Cardenal J, Gómez JM, Colomo C, Delgado J (2016) Analysis of landslide evolution affecting olive groves using UAV and photogrammetric techniques. Remote Sens 8(10):837
65. Franz TE, Wahbi A, Vreugdenhil M, Weltin G, Heng L, Oismueller M, Strauss P, Dercon G, Desilets D (2016) Using cosmic-ray neutron probes to monitor landscape scale soil water content in mixed land use agricultural systems. Appl Environ Soil Sci 2016
66. Freeman PK, Freeland RS (2016) Media framing the reception of unmanned aerial vehicles in the United States of America. Technol Soc 44:23–29
67. Gago J, Douthe C, Coopman R, Gallego P, Ribas-Carbo M, Flexas J, Escalona J, Medrano H (2015) UAVs challenge to assess water stress for sustainable agriculture. Agric Water Manag 153:9–19
68. Galvao L, Ponzoni F, Epiphanio J, Rudorff B, Formaggio A (2004) Sun and view angle effects on NDVI determination of land cover types in the Brazilian Amazon region with hyperspectral data. Int J Remote Sens 25(10):1861–1879
69. Gebbers R (2019) proximal soil surveying and monitoring techniques, chap 2. Burleigh Dodds Science Publishing, Cambridge, pp 29–77
70. Gebbers R, Lück E, Dabas M, Domsch H (2009) Comparison of instruments for geoelectrical soil mapping at the field scale. Near Surface Geophysics 7(3):179–190
71. Geipel J, Link J, Claupein W (2014) Combined spectral and spatial modeling of corn yield based on aerial images and crop surface models acquired with an unmanned aircraft system. Remote Sens 6(11):10335–10355
72. Gonzalez-Dugo V, Zarco-Tejada P, Nicolás E, Nortes PA, Alarcón J, Intrigliolo DS, Fereres E (2013) Using high resolution UAV thermal imagery to assess the variability in the water status of five fruit tree species within a commercial orchard. Precis Agric 14(6):660–678
73. Green RO, Eastwood ML, Sarture CM, Chrien TG, Aronsson M, Chippendale BJ, Faust JA, Pavri BE, Chovit CJ, Solis M et al (1998) Imaging spectroscopy and the airborne visible/infrared imaging spectrometer (AVIRIS). Remote Sens Environ 65(3):227–248
74. Haghighattalab A, Pérez LG, Mondal S, Singh D, Schinstock D, Rutkoski J, Ortiz-Monasterio I, Singh RP, Goodin D, Poland J (2016) Application of unmanned aerial systems for high throughput phenotyping of large wheat breeding nurseries. Plant Methods 12(1):35
75. Hannam JA, Van Dam RL, Harmon RS (2020) Emerging applications and new frontiers: report
76. Heggemann T, Welp G, Amelung W, Angst G, Franz SO, Koszinski S, Schmidt K, Pätzold S (2017) Proximal gamma-ray spectrometry for site-independent in situ prediction of soil texture on ten heterogeneous fields in Germany using support vector machines. Soil Tillage Res 168:99–109
77. Heil K, Schmidhalter U (2017) The application of EM38: determination of soil parameters, selection of soil sampling points and use in agriculture and archaeology. Sensors 17(11):2540
78. Hemmat A, Adamchuk V (2008) Sensor systems for measuring spatial variation in soil compaction. Comput Electron Agric 63(2):89–103
79. Hillnhütter C, Mahlein AK, Sikora RA, Oerke EC (2012) Use of imaging spectroscopy to discriminate symptoms caused by Heterodera schachtii and Rhizoctonia solani on sugar beet. Precis Agric 13(1):17–32
80. Hirakawa K, Wolfe PJ (2018) Spatio-spectral sampling and color filter array design. In: Single-sensor imaging. CRC Press, Boca Raton, pp 157–172
81. Hoffmann H, Jensen R, Thomsen A, Nieto H, Rasmussen J, Friborg T (2016) Crop water stress maps for an entire growing season from visible and thermal UAV imagery. Biogeosciences 13, 6545–6563
82. Holland K, Schepers J (2010) Derivation of a variable rate nitrogen application model for in-season fertilization of corn. Agron J 102(5):1415–1424

83. Holland KH, Schepers JS (2013) Use of a virtual-reference concept to interpret active crop canopy sensor data. Precis Agric 14(1):71–85
84. Holland KH, Lamb DW, Schepers JS (2012) Radiometry of proximal active optical sensors (AOS) for agricultural sensing. IEEE J Sel Top Appl Earth Obs Remote Sens 5(6):1793–1802
85. Holland Scientific - NVDI Sensors (2020). https://hollandscientific.com/
86. Holman FH, Riche AB, Michalski A, Castle M, Wooster MJ, Hawkesford MJ (2016) High throughput field phenotyping of wheat plant height and growth rate in field plot trials using UAV based remote sensing. Remote Sens 8(12):1031
87. Home (2020). https://agriculture.trimble.com/
88. Hunt ER, Cavigelli M, Daughtry CS, Mcmurtrey JE, Walthall CL (2005) Evaluation of digital photography from model aircraft for remote sensing of crop biomass and nitrogen status. Precis Agric 6(4):359–378
89. Hunt ER, Hively WD, Fujikawa SJ, Linden DS, Daughtry CS, McCarty GW (2010) Acquisition of NIR-green-blue digital photographs from unmanned aircraft for crop monitoring. Remote Sens 2(1):290–305
90. Inoue M, Ahmed BO, Saito T, Irshad M (2008) Comparison of twelve dielectric moisture probes for soil water measurement under saline conditions. Am J Environ Sci 4(4):367–372
91. Irmak S, Irmak A (2005) Performance of frequency-domain reflectometer, capacitance, and psuedo-transit time-based soil water content probes in four coarse-textured soils. Appl Eng Agric 21(6):999–1008
92. Irmak S, Rees JM, Zoubek GL, van DeWalle BS, Rathje WR, DeBuhr R, Leininger D, Siekman DD, Schneider JW, Christiansen AP (2010) Nebraska agricultural water management demonstration network (NAWMDN): integrating research and extension/outreach. Appl Eng Agric 26(4):599–613
93. Jenny H (2012) The soil resource: origin and behavior, vol 37. Springer Science & Business Media, Berlin
94. Käthner J, Ben-Gal A, Gebbers R, Peeters A, Herppich WB, Zude-Sasse M (2017) Evaluating spatially resolved influence of soil and tree water status on quality of European plum grown in semi-humid climate. Front Plant Sci 8:1053
95. Kaur J, Adamchuk VI, Whalen JK, Ismail AA (2015) Development of an NDIR CO2 sensor-based system for assessing soil toxicity using substrate-induced respiration. Sensors 15(3):4734–4748
96. Khanal S, Fulton J, Shearer S (2017) An overview of current and potential applications of thermal remote sensing in precision agriculture. Comput Electron Agric 139:22–32
97. Kim HJ, Sudduth KA, Hummel JW (2009) Soil macronutrient sensing for precision agriculture. J Environ Monit 11(10):1810–1824
98. King DJ (1995) Airborne multispectral digital camera and video sensors: a critical review of system designs and applications. Can J Remote Sens 21(3):245–273
99. Knödel K, Krummel H, Lange G (2013) Handbuch zur Erkundung des Untergrundes von Deponien und Altlasten: Band 3: Geophysik. Springer, Berlin
100. Konda A, Rau A, Stoller MA, Taylor JM, Salam A, Pribil GA, Argyropoulos C, Morin SA (2018) Soft microreactors for the deposition of conductive metallic traces on planar, embossed, and curved surfaces. Adv Funct Mater 28(40):1803020. https://doi.org/10.1002/adfm.201803020
101. Kukal MS, Irmak S, Sharma K et al (2019) Development and application of a performance and operational feasibility guide to facilitate adoption of soil moisture sensors. Sustainability 12(1):1–19
102. Kuras O, Beamish D, Meldrum PI, Ogilvy RD (2006) Fundamentals of the capacitive resistivity technique. Geophysics 71(3):G135–G152
103. Lamb D, Schneider D, Stanley J (2014) Combination active optical and passive thermal infrared sensor for low-level airborne crop sensing. Precis Agric 15(5):523–531
104. Lee K, Ehsani R (2009) A laser scanner based measurement system for quantification of citrus tree geometric characteristics. Appl Eng Agric 25(5):777–788

105. Lesmes DP, Friedman SP (2005) Relationships between the electrical and hydrogeological properties of rocks and soils. In: Hydrogeophysics. Springer, Berlin, pp 87–128
106. Li Z, Isler V (2016) Large scale image mosaic construction for agricultural applications. IEEE Robot Autom Lett 1(1):295–302
107. Li Y, Zhang M, Zheng J, Pan L, Kong P, Lei Z (2017) Design and experiment of prototype soil pretreatment device for ISE-based soil nitrate-nitrogen detection. Trans Chin Soc Agric Eng 33(1):120–125
108. Long DS, McCallum JD (2015) On-combine, multi-sensor data collection for post-harvest assessment of environmental stress in wheat. Precis Agric 16(5):492–504
109. López-Granados F (2011) Weed detection for site-specific weed management: mapping and real-time approaches. Weed Res 51(1):1–11
110. Lucieer A, Malenovskỳ Z, Veness T, Wallace L (2014) HyperUAS—imaging spectroscopy from a multirotor unmanned aircraft system. J Field Robot 31(4):571–590
111. Lueck E, Rühlmann J (2013) Resistivity mapping with geophilus electricus—information about lateral and vertical soil heterogeneity. Geoderma 199:2–11
112. Mahmood HS, Hoogmoed WB, Van Henten EJ (2013) Proximal gamma-ray spectroscopy to predict soil properties using windows and full-spectrum analysis methods. Sensors 13(12):16263–16280
113. Markwell J, Osterman JC, Mitchell JL (1995) Calibration of the Minolta SPAD-502 leaf chlorophyll meter. Photosynth Res 46(3):467–472
114. Martins CH, Alshehri AA, Akyildiz IF (2017) Novel MI-based (FracBot) sensor hardware design for monitoring hydraulic fractures and oil reservoirs. In: 2017 IEEE 8th annual ubiquitous computing, electronics and mobile communication conference (UEMCON). IEEE, Piscataway, pp 434–441
115. Mausel P, Everitt J, Escobar D, King D (1992) Airborne videography: current status and future perspectives. Photogramm Eng Remote Sensing 58(8):1189–1195
116. McNeill J (1980) Electromagnetic terrain conductivity measurement at low induction numbers. Geonics Ltd., Mississauga
117. Metternicht G, Zinck J (2003) Remote sensing of soil salinity: potentials and constraints. Remote Sens Environ 85(1):1–20
118. Minolta K (2009) Chlorophyll meter SPAD-502plus. Konica Minolta
119. Mohamed A (2008) Impact of soil magnetic permeability on water content prediction using TDR. In: The 12th international conference of international association for computer methods and advances in geomechanics (IACMAG), Citeseer
120. Moran MS, Inoue Y, Barnes E (1997) Opportunities and limitations for image-based remote sensing in precision crop management. Remote Sens Environ 61(3):319–346
121. Muñoz-Carpena R, Shukla S, Morgan K (2004) Field devices for monitoring soil water content, vol 343. University of Florida Cooperative Extension Service, Institute of Food and Agricultural Sciences
122. Nex F, Remondino F (2014) UAV for 3d mapping applications: a review. Appl Geomat 6(1):1–15
123. Nijland W, De Jong R, De Jong SM, Wulder MA, Bater CW, Coops NC (2014) Monitoring plant condition and phenology using infrared sensitive consumer grade digital cameras. Agric For Meteorol 184:98–106
124. Ochsner TE, Cosh MH, Cuenca RH, Dorigo WA, Draper CS, Hagimoto Y, Kerr YH, Njoku EG, Small EE, Zreda M (2013) State of the art in large-scale soil moisture monitoring. Soil Sci Soc Am J 77(6):1888–1919
125. Pan Z, Lie D, Qiang L, Shaolan H, Shilai Y, Yande L, Yongxu Y, Haiyang P (2016) Effects of citrus tree-shape and spraying height of small unmanned aerial vehicle on droplet distribution. Int J Agric Biol Eng 9(4):45–52
126. Panciera R, Walker JP, Jackson TJ, Gray DA, Tanase MA, Ryu D, Monerris A, Yardley H, Rudiger C, Wu X et al (2014) The soil moisture active passive experiments (SMAPEx): toward soil moisture retrieval from the SMAP mission. IEEE Trans Geosci Remote Sens 52(1):490–507

127. Peña JM, Torres-Sánchez J, de Castro AI, Kelly M, López-Granados F (2013) Weed mapping in early-season maize fields using object-based analysis of unmanned aerial vehicle (UAV) images. PLoS ONE 8(10), e77151
128. Pérez-Ortiz M, Peña J, Gutiérrez PA, Torres-Sánchez J, Hervás-Martínez C, López-Granados F (2015) A semi-supervised system for weed mapping in sunflower crops using unmanned aerial vehicles and a crop row detection method. Appl Soft Comput 37:533–544
129. Quinones H, Ruelle P, Nemeth I (2003) Comparison of three calibration procedures for TDR soil moisture sensors. Irrig Drain 52(3):203–217
130. Rabatel G, Gorretta N, Labbe S (2014) Getting simultaneous red and near-infrared band data from a single digital camera for plant monitoring applications: theoretical and practical study. Biosyst Eng 117:2–14
131. Rasmussen J, Ntakos G, Nielsen J, Svensgaard J, Poulsen RN, Christensen S (2016) Are vegetation indices derived from consumer-grade cameras mounted on UAVs sufficiently reliable for assessing experimental plots? Eur J Agron 74:75–92
132. Raun WR, Solie JB, Johnson GV, Stone ML, Mullen RW, Freeman KW, Thomason WE, Lukina EV (2002) Improving nitrogen use efficiency in cereal grain production with optical sensing and variable rate application. Agron J 94(4):815–820
133. Reece CF (1996) Evaluation of a line heat dissipation sensor for measuring soil matric potential. Soil Sci Soc Am J 60(4):1022–1028
134. Risinger M, Carver K (2020) Neutron moisture meters. http://sanangelo.tamu.edu/extension/agronomy/agronomy-publications/grain-sorghum-production-in-west-central-texas/how-to-estimate-soil-moisture-by-feel/soil-moisture-measuring-devices/neutron-moisture-meters/
135. Robinson D, Jones SB, Wraith J, Or D, Friedman S (2003) A review of advances in dielectric and electrical conductivity measurement in soils using time domain reflectometry. Vadose Zone J 2(4):444–475
136. Roldán JJ, Joossen G, Sanz D, Del Cerro J, Barrientos A (2015) Mini-UAV based sensory system for measuring environmental variables in greenhouses. Sensors 15(2):3334–3350
137. Rossel RV, Adamchuk V, Sudduth K, McKenzie N, Lobsey C (2011) Proximal soil sensing: an effective approach for soil measurements in space and time. In: Advances in agronomy, vol 113. Elsevier, Amsterdam, pp 243–291
138. Rouse J, Haas R, Schell J, Deering D (1974) Monitoring vegetation systems in the great plains with ERTS. NASA Spec Publ 351:309
139. Rudnick DR, Djaman K, Irmak S (2015) Performance analysis of capacitance and electrical resistance-type soil moisture sensors in a silt loam soil. Trans ASABE 58(3):649–665
140. Sakamoto T, Gitelson AA, Nguy-Robertson AL, Arkebauer TJ, Wardlow BD, Suyker AE, Verma SB, Shibayama M (2012) An alternative method using digital cameras for continuous monitoring of crop status. Agric For Meteorol 154:113–126
141. Salam A (2018) Pulses in the sand: long range and high data rate communication techniques for next generation wireless underground networks. ETD collection for University of Nebraska - Lincoln (AAI10826112), http://digitalcommons.unl.edu/dissertations/AAI10826112
142. Salam A (2019) A comparison of path loss variations in soil using planar and dipole antennas. In: 2019 IEEE international symposium on antennas and propagation. IEEE, Piscataway
143. Salam A (2019) Design of subsurface phased array antennas for digital agriculture applications. In: Proc. 2019 IEEE international symposium on phased array systems and technology (IEEE Array 2019), Waltham, MA
144. Salam A (2019) A path loss model for through the soil wireless communications in digital agriculture. In: 2019 IEEE international symposium on antennas and propagation. IEEE, Piscataway, pp 1–2
145. Salam A (2019) Sensor-free underground soil sensing. In: ASA, CSSA and SSSA international annual meetings, ASA-CSSA-SSSA
146. Salam A (2019) Subsurface MIMO: a beamforming design in internet of underground things for digital agriculture applications. J. Sens. Actuator Netw. 8(3). https://doi.org/10.3390/jsan8030041, https://www.mdpi.com/2224-2708/8/3/41

147. Salam A (2019) Underground environment aware MIMO design using transmit and receive beamforming in internet of underground things. Springer International Publishing, Cham, pp 1–15
148. Salam A (2019) An underground radio wave propagation prediction model for digital agriculture. Information 10(4):147
149. Salam A (2019) Underground soil sensing using subsurface radio wave propagation. In: 5th global workshop on proximal soil sensing, Columbia, MO
150. Salam A (2020) Internet of things for environmental sustainability and climate change. Springer International Publishing, Cham, pp 33–69. https://doi.org/10.1007/978-3-030-35291-2_2
151. Salam A (2020) Internet of things for sustainability: perspectives in privacy, cybersecurity, and future trends. Springer International Publishing, Cham, pp 299–327. https://doi.org/10.1007/978-3-030-35291-2_10
152. Salam A (2020) Internet of things for sustainable community development, 1st edn. Springer Nature, Berlin. https://doi.org/10.1007/978-3-030-35291-2
153. Salam A (2020) Internet of things for sustainable community development: introduction and overview. Springer International Publishing, Cham, pp 1–31. https://doi.org/10.1007/978-3-030-35291-2_1
154. Salam A (2020) Internet of things for sustainable forestry. Springer International Publishing, Cham, pp 147–181. https://doi.org/10.1007/978-3-030-35291-2_5
155. Salam A (2020) Internet of things for sustainable human health. Springer International Publishing, Cham, pp 217–242. https://doi.org/10.1007/978-3-030-35291-2_7
156. Salam A (2020) Internet of things for sustainable mining. Springer International Publishing, Cham, pp 243–271. https://doi.org/10.1007/978-3-030-35291-2_8
157. Salam A (2020) Internet of things for water sustainability. Springer International Publishing, Cham, pp 113–145. https://doi.org/10.1007/978-3-030-35291-2_4
158. Salam A (2020) Internet of things in agricultural innovation and security. Springer International Publishing, Cham, pp 71–112. https://doi.org/10.1007/978-3-030-35291-2_3
159. Salam A (2020) Internet of things in sustainable energy systems. Springer International Publishing, Cham, pp 183–216. https://doi.org/10.1007/978-3-030-35291-2_6
160. Salam A (2020) Internet of things in water management and treatment. Springer International Publishing, Cham, pp 273–298. https://doi.org/10.1007/978-3-030-35291-2_9
161. Salam A (2020) Wireless underground communications in sewer and stormwater overflow monitoring: radio waves through soil and asphalt medium. Information 11(2), 98
162. Salam A, Karabiyik U (2019) A cooperative overlay approach at the physical layer of cognitive radio for digital agriculture. In: Proceedings of the 3rd international Balkan conference on communications and networking (2019 BalkanCom)
163. Salam A, Shah S (2019) Internet of things in smart agriculture: enabling technologies. In: 2019 IEEE 5th world forum on internet of things (WF-IoT). IEEE, Piscataway, pp 692–695
164. Salam A, Vuran MC (2016) Impacts of soil type and moisture on the capacity of multi-carrier modulation in internet of underground things. In: Proc. of the 25th ICCCN 2016, Waikoloa, Hawaii
165. Salam A, Vuran MC (2017) EM-based wireless underground sensor networks, pp 247–285. https://doi.org/10.1016/B978-0-12-803139-1.00005-9
166. Salam A, Vuran MC (2017) Smart underground antenna arrays: a soil moisture adaptive beamforming approach. In: Proc. IEEE INFOCOM 2017, Atlanta
167. Salam A, Vuran MC (2017) Wireless underground channel diversity reception with multiple antennas for internet of underground things. In: Proc. IEEE ICC 2017, Paris
168. Salam A, Vuran MC, Irmak S (2016) Pulses in the sand: impulse response analysis of wireless underground channel. In: The 35th annual IEEE international conference on computer communications (INFOCOM 2016), San Francisco
169. Salam A, Vuran MC, Irmak S (2017) Towards internet of underground things in smart lighting: a statistical model of wireless underground channel. In: Proc. 14th IEEE international conference on networking, sensing and control (IEEE ICNSC), Calabria

170. Salam A, Hoang AD, Meghna A, Martin DR, Guzman G, Yoon YH, Carlson J, Kramer J, Yansi K, Kelly M et al (2019) The future of emerging IoT paradigms: architectures and technologies. https://doi.org/10.20944/preprints201912.0276.v1
171. Salam A, Vuran MC, Dong X, Argyropoulos C, Irmak S (2019) A theoretical model of underground dipole antennas for communications in internet of underground things. IEEE Trans Antennas Propag. https://doi.org/10.1109/TAP.2019.2902646
172. Salam A, Vuran MC, Irmak S (2019) Di-sense: in situ real-time permittivity estimation and soil moisture sensing using wireless underground communications. Comput Netw 151:31–41. https://doi.org/10.1016/j.comnet.2019.01.001, http://www.sciencedirect.com/science/article/pii/S1389128618303141
173. Samborski SM, Tremblay N, Fallon E (2009) Strategies to make use of plant sensors-based diagnostic information for nitrogen recommendations. Agron J 101(4):800–816
174. Samouëlian A, Cousin I, Tabbagh A, Bruand A, Richard G (2005) Electrical resistivity survey in soil science: a review. Soil Tillage Res 83(2):173–193
175. Sankaran S, Ehsani R (2012) Detection of huanglongbing disease in citrus using fluorescence spectroscopy. Trans ASABE 55(1):313–320
176. Sankaran S, Khot LR, Carter AH (2015) Field-based crop phenotyping: multispectral aerial imaging for evaluation of winter wheat emergence and spring stand. Comput Electron Agric 118:372–379
177. Sankaran S, Khot LR, Espinoza CZ, Jarolmasjed S, Sathuvalli VR, Vandemark GJ, Miklas PN, Carter AH, Pumphrey MO, Knowles NR et al (2015) Low-altitude, high-resolution aerial imaging systems for row and field crop phenotyping: a review. Eur J Agron 70:112–123
178. Santamarina JC, Rinaldi VA, Fratta D, Klein KA, Wang YH, Cho GC, Cascante G (2005) A survey of elastic and electromagnetic properties of near-surface soils. Near-Surface Geophys 1:71–87
179. Scharf PC, Brouder SM, Hoeft RG (2006) Chlorophyll meter readings can predict nitrogen need and yield response of corn in the North-Central USA. Agron J 98(3):655–665
180. Schirrmann M, Giebel A, Gleiniger F, Pflanz M, Lentschke J, Dammer KH (2016) Monitoring agronomic parameters of winter wheat crops with low-cost UAV imagery. Remote Sens 8(9):706
181. Selsam P, Schaeper W, Brinkmann K, Buerkert A (2017) Acquisition and automated rectification of high-resolution RGB and near-IR aerial photographs to estimate plant biomass and surface topography in arid agro-ecosystems. Exp Agric 53(1):144–157
182. Sepúlveda-Reyes D, Ingram B, Bardeen M, Zúñiga M, Ortega-Farías S, Poblete-Echeverría C (2016) Selecting canopy zones and thresholding approaches to assess grapevine water status by using aerial and ground-based thermal imaging. Remote Sens 8(10):822
183. Severtson D, Callow N, Flower K, Neuhaus A, Olejnik M, Nansen C (2016) Unmanned aerial vehicle canopy reflectance data detects potassium deficiency and green peach aphid susceptibility in canola. Precis Agric 17(6):659–677
184. Shamal S, Alhwaimel SA, Mouazen AM (2016) Application of an on-line sensor to map soil packing density for site specific cultivation. Soil Tillage Res 162:78–86
185. Shi Y, Thomasson JA, Murray SC, Pugh NA, Rooney WL, Shafian S, Rajan N, Rouze G, Morgan CL, Neely HL et al (2016) Unmanned aerial vehicles for high-throughput phenotyping and agronomic research. PloS ONE 11(7). https://doi.org/10.1371/journal.pone.0159781
186. Shiratsuchi L, Ferguson R, Shanahan J, Adamchuk V, Rundquist D, Marx D, Slater G (2011) Water and nitrogen effects on active canopy sensor vegetation indices. Agron J 103(6):1815–1826
187. Slaughter D, Giles D, Downey D (2008) Autonomous robotic weed control systems: a review. Comput Electron Agric 61(1):63–78
188. Smith M, Carrivick J, Quincey D (2016) Structure from motion photogrammetry in physical geography. Prog Phys Geogr 40(2):247–275
189. Smolka M, Puchberger-Enengl D, Bipoun M, Klasa A, Kiczkajlo M, Śmiechowski W, Sowiński P, Krutzler C, Keplinger F, Vellekoop M (2017) A mobile lab-on-a-chip device for on-site soil nutrient analysis. Precis Agric 18(2):152–168

190. Stafford J, Hendrick J (1988) Dynamic sensing of soil pans. Trans ASAE 31(1):9–0013
191. Steinberg S, van Bavel CH, McFarland MJ (1989) A gauge to measure mass flow rate of sap in stems and trunks of woody plants. J Am Soc Hortic Sci 114(3):466–472
192. Stiekema H (2012) The Ag leader OptRx crop sensor. Ag Leader Technology Inc, Ag Leader Europe bv
193. Sudduth KA, Kitchen N, Bollero G, Bullock D, Wiebold W (2003) Comparison of electromagnetic induction and direct sensing of soil electrical conductivity. Agron J 95(3):472–482
194. Sugiura R, Noguchi N, Ishii K (2007) Correction of low-altitude thermal images applied to estimating soil water status. Biosyst Eng 96(3):301–313
195. Sui R, Thomasson JA, Hanks J, Wooten J (2008) Ground-based sensing system for weed mapping in cotton. Comput Electron Agric 60(1):31–38
196. Teal R, Tubana B, Girma K, Freeman K, Arnall D, Walsh O, Raun W (2006) In-season prediction of corn grain yield potential using normalized difference vegetation index. Agron J 98(6):1488–1494
197. Temel S, Vuran MC, Lunar MM, Zhao Z, Salam A, Faller RK, Stolle C (2018) Vehicle-to-barrier communication during real-world vehicle crash tests. Comput Commun 127:172–186
198. Thomsen A, Schelde K, Drøscher P, Steffensen F (2007) Mobile TDR for geo-referenced measurement of soil water content and electrical conductivity. Precis Agric 8(4-5):213–223
199. Tilly N, Hoffmeister D, Cao Q, Huang S, Lenz-Wiedemann V, Miao Y, Bareth G (2014) Multitemporal crop surface models: accurate plant height measurement and biomass estimation with terrestrial laser scanning in paddy rice. J Appl Remote Sens 8(1):083671
200. Torres-Sánchez J, Peña JM, de Castro AI, López-Granados F (2014) Multi-temporal mapping of the vegetation fraction in early-season wheat fields using images from UAV. Comput Electron Agric 103:104–113
201. Torres-Sánchez J, Lopez-Granados F, Serrano N, Arquero O, Peña JM (2015) High-throughput 3-D monitoring of agricultural-tree plantations with unmanned aerial vehicle (UAV) technology. PloS ONE 10(6). https://doi.org/10.1371/journal.pone.0130479
202. Tremblay N, Wang Z, Ma BL, Belec C, Vigneault P (2009) A comparison of crop data measured by two commercial sensors for variable-rate nitrogen application. Precis Agric 10(2):145
203. Tuller M, Islam MR (2005) Field methods for monitoring solute transport. CRC Press, Boca Raton, FL
204. UC of Agriculture (2018) Irrigation and water management survey. https://www.nass.usda.gov/Publications/AgCensus/2017/Online_Resources/Farm_and_Ranch_Irrigation_Survey/fris.pdf
205. Uto K, Seki H, Saito G, Kosugi Y (2013) Characterization of rice paddies by a UAV-mounted miniature hyperspectral sensor system. IEEE J Sel Top Appl Earth Obs Remote Sens 6(2):851–860
206. Van Egmond F, Loonstra E, Limburg J (2010) Gamma ray sensor for topsoil mapping: the mole. In: Proximal soil sensing. Springer, Berlin, pp 323–332
207. Vereecken H, Huisman J, Pachepsky Y, Montzka C, Van Der Kruk J, Bogena H, Weihermüller L, Herbst M, Martinez G, Vanderborght J (2014) On the spatio-temporal dynamics of soil moisture at the field scale. J Hydrol 516:76–96
208. Verger A, Vigneau N, Chéron C, Gilliot JM, Comar A, Baret F (2014) Green area index from an unmanned aerial system over wheat and rapeseed crops. Remote Sens Environ 152:654–664
209. Veris Technology (2020). https://www.veristech.com/the-sensors/v3100
210. Vuran MC, Salam A, Wong R, Irmak S (2018) Internet of underground things in precision agriculture: architecture and technology aspects. Ad Hoc Netw. https://doi.org/10.1016/j.adhoc.2018.07.017, http://www.sciencedirect.com/science/article/pii/S1570870518305067
211. Vuran MC, Salam A, Wong R, Irmak S (2018) Internet of underground things: sensing and communications on the field for precision agriculture. In: 2018 IEEE 4th world forum on internet of things (WF-IoT) (WF-IoT 2018), Singapore

212. Wallihan E (1973) Portable reflectance meter for estimating chlorophyll concentrations in leaves 1. Agron J 65(4):659–662
213. Weis M, Andújar D, Peteinatos G, Gerhards R (2013) Improving the determination of plant characteristics by fusion of four different sensors. In: Precision agriculture'13. Springer, Berlin, pp 63–69
214. Whitehead K, Hugenholtz CH (2014) Remote sensing of the environment with small unmanned aircraft systems (UASS), part 1: a review of progress and challenges. J Unmanned Veh Syst 2(3):69–85
215. Willkomm M, Bolten A, Bareth G (2016) Non-destructive monitoring of rice by hyperspectral in-field spectrometry and UAV-based remote sensing: case study of field-grown rice in North Rhine-Westphalia, vol 41. International Archives of the Photogrammetry, Remote Sensing & Spatial Information Sciences
216. Wilson AD, Baietto M (2009) Applications and advances in electronic-nose technologies. Sensors 9(7):5099–5148
217. Wu M, Yang C, Song X, Hoffmann WC, Huang W, Niu Z, Wang C, Li W (2017) Evaluation of orthomosics and digital surface models derived from aerial imagery for crop type mapping. Remote Sens 9(3):239
218. Yang C (2012) A high-resolution airborne four-camera imaging system for agricultural remote sensing. Comput Electron Agric 88:13–24
219. Yang C, Hoffmann WC (2015) Low-cost single-camera imaging system for aerial applicators. J Appl Remote Sens 9(1):096064
220. Yang C, Everitt JH, Bradford JM, Murden D (2004) Airborne hyperspectral imagery and yield monitor data for mapping cotton yield variability. Precis Agric 5(5):445–461
221. Yang C, Everitt JH, Du Q, Luo B, Chanussot J (2012) Using high-resolution airborne and satellite imagery to assess crop growth and yield variability for precision agriculture. Proc IEEE 101(3):582–592
222. Yang C, Westbrook JK, Suh CPC, Martin DE, Hoffmann WC, Lan Y, Fritz BK, Goolsby JA (2014) An airborne multispectral imaging system based on two consumer-grade cameras for agricultural remote sensing. Remote Sens 6(6):5257–5278
223. Yara International (2018) Yara publishes 2017 Annual Report. https://www.yara.com/corporate-releases/yara-publishes-2017-annual-report/
224. Zarco-Tejada PJ, González-Dugo V, Berni JA (2012) Fluorescence, temperature and narrow-band indices acquired from a UAV platform for water stress detection using a micro-hyperspectral imager and a thermal camera. Remote Sens Environ 117:322–337
225. Zarco-Tejada PJ, Diaz-Varela R, Angileri V, Loudjani P (2014) Tree height quantification using very high resolution imagery acquired from an unmanned aerial vehicle (UAV) and automatic 3d photo-reconstruction methods. Eur J Agron 55:89–99
226. Zebarth B, Rees H, Tremblay N, Fournier P, Leblon B (2002) Mapping spatial variation in potato nitrogen status using the N sensor. In: XXVI international horticultural congress: toward ecologically sound fertilization strategies for field vegetable production 627, pp 267–273
227. Zhang C, Walters D, Kovacs JM (2014) Applications of low altitude remote sensing in agriculture upon farmers' requests–a case study in northeastern Ontario, Canada. PLoS ONE 9(11):e112894
228. Zhou J, Khot LR, Peters T, Whiting MD, Zhang Q, Granatstein D (2016) Efficacy of unmanned helicopter in rainwater removal from cherry canopies. Comput Electron Agric 124:161–167
229. Zhu Y, Irmak S, Jhala AJ, Vuran MC, Diotto A (2019) Time-domain and frequency-domain reflectometry type soil moisture sensor performance and soil temperature effects in fine-and coarse-textured soils. Appl Eng Agric 35(2):117–134